E.T.S. de Ingeniería Industrial,
Informática y de Telecomunicación

Vibrational sensor based on Giant Magnetoimpedance effect

Bachelor's Degree

in Industrial Engineering

Final Year Project

Author: Aitor Ballano Biurrun

Directors: Cristina Gómez Polo y Juan Jesús Beato López

Pamplona a 21/05/2020

upna Universidad Pública de Navarra
Nafarroako Unibertsitate Publikoa

Abstract and key words

The main purpose of this work is to explore the use of the Giant Magneto Impedance effect (*GMI*) in a sensor to detect low frequency vibrations of moving objects. This effect is characterized by huge variations of the high frequency electric impedance of a soft magnetic conductor under the action of an external magnetic field. Thus, the detection principle is based on the characterisation of the magnetic field generated by a permanent magnet attached to the object under movement (vibration).

Before analysing the configuration of the sensor, it was necessary to study different materials to be employed as sensor nucleus. This previous characterization enabled to select the material with optimum response (maximum impedance variation) and to determine the optimum operation conditions. These two main parameters which were studied are: frequency and current. In order to obtain the best sensor's response, it must be powered with the optimum values of frequency and current.

Once the optimum parameters of the exciting frequency were determined, the response of the sensor was studied for several vibration frequencies and under certain conditions.

The keywords of this project are the following:

- Sensor.
- Giant magnetoimpedance.
- Accelerometer.
- Ribbon.
- Wire.
- Frequency.
- Current.

Contents

Introduction 5
Objectives 8
Methodology 9
Characterization of the samples as a function of the frequency and amplitude of the electric current 9
Characterization of the samples under a static magnetic field 11
Variation of the voltage of the sample with the distance to the magnet 11
Characterization of the selected sample under a vibrating magnetic field 14
Results and analysis of the work. 17
First phase: Selection of the sample 17
Characterization of the wire in frequency and amplitude of the current 17
Characterization of the ribbon in frequency and amplitude of the current 19
Variation of the voltage of the wire of 3 cm with the distance to the magnet 21
Variation of the voltage of the ribbon of 3 cm with the distance to the magnet 23
Variation of the voltage of the ribbon of 7 cm with the distance to the magnet 25
Conclusions of the first phase 26
Second phase: Characterization of the shaker with the magnet. 27
Conclusions 34
Bibliography 35
Annex charts 36

Introduction

Nowadays magnetic sensors play an important role in technology. Widespread, they are used in practically each sector, industrial sector, engineering, military, space research, bio magnetic measurements for medicine and so on. There is a huge variety of them such as induction sensors, Hall effect magnetic sensors, magneto-optical sensors, Giant Magneto Resistive sensors…

The operation principle of these sensors is to correlate the magnetic field to a voltage or impedance. Each sensor has different operating element and its applications may vary from measuring field gradients to applications of non-contact switching. [1]

The discovery of the Giant Magneto Impedance (*GMI*) effect has helped to the development of high-performance magnetic sensors. This effect is characterized by huge changes in the high frequency electric impedance of a soft magnetic conductor under the action of an external magnetic field. New alloys have been designed in order to obtain maximum changes in the *ac* impedance when subjected to an applied magnetic field (H_{dc}). Other advantages of this kind of sensors are high flexibility, low prices and last but not least the ultra-high sensitivity which would make them widely employed in the design of sensors for different technological applications (compasses, non-contact position sensors).

To understand the concept of *GMI* we take a soft ferromagnetic conductor and we apply a magnetic field on it. If a small alternating current (*ac*) flows through the conductor the *ac* complex impedance, *Z*, of the sample will suffer a large change. To characterize impedance variations, *GMI* ratio is usually defined as:

$$\frac{\Delta Z}{Z}(\%) = 100\%\, x\, \frac{Z(H_{dc}) - Z(H_{max})}{Z(H_{max})} \qquad (1)$$

Being H_{max} the magnetic field applied in order to saturate the impedance of our magnetic material. The complex impedance is defined as the sum of the real (*R*) and complex (*X*) part ($Z = R + iX$), where the real part is the resistive element and the *X* is the inductance of the material. This complex impedance is obtained by V_{ac}/I_{ac}, where V_{ac} is the voltage drop between the ends of the conductor and I_{ac} is the ac current flowing through it [3],[4]. (See Figure 1)

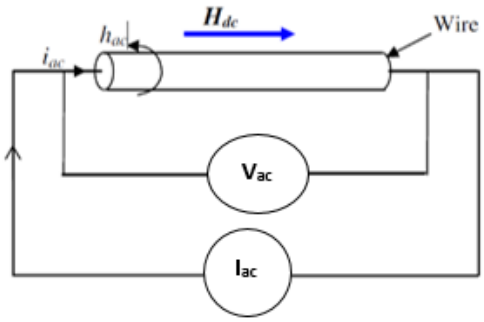

Figure 1 Schematic of the sample powered by an ac current.

In Figure 2 is shown a typical magnetoimpedance response, that is, the sharp decrease of *Z* under the action of an external magnetic field.

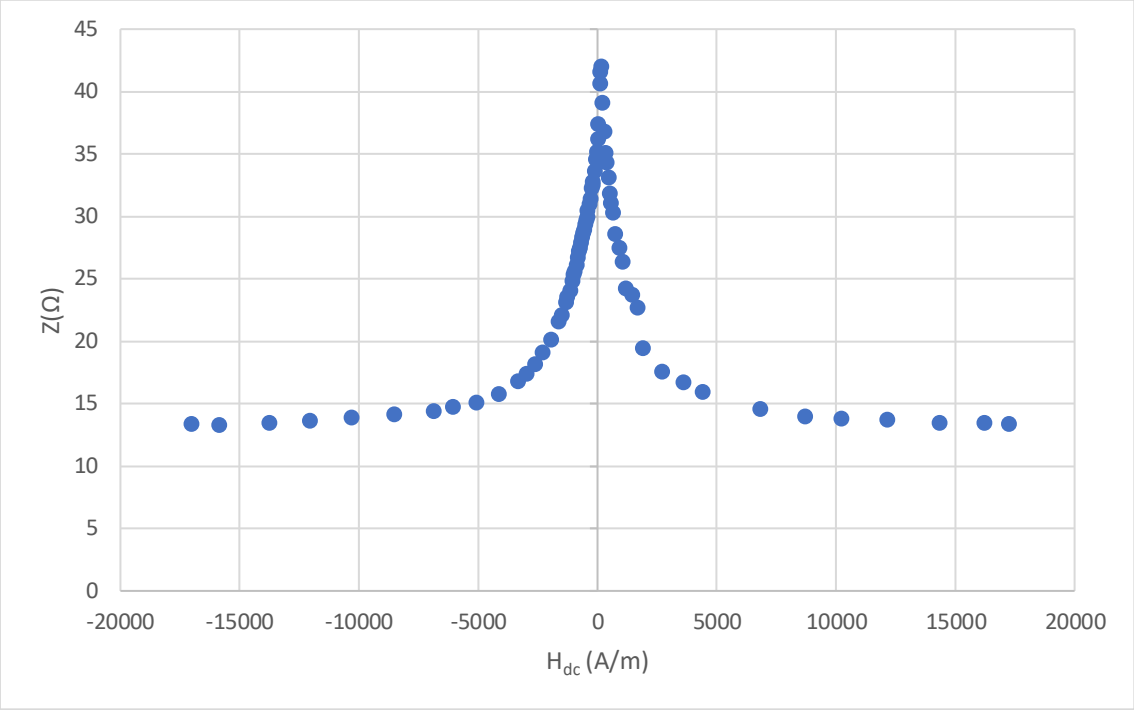

Figure 2 Impedance, Z, as a function of the magnetic field, H_{dc}, for a wire (19,5 mA and 400 kHz, amplitude and frequency current).

The changes in *Z* can be understood in terms of the skin effect, δ_m defined as:

$$\delta_m = \frac{c}{\sqrt{4\Pi^2 f \sigma \mu}} \qquad (2)$$

Where f is the frequency of excitation and μ the magnetic permeability associated to the magnetization process driven by magnetic field associated to the current flow.

For a given *ac* current flowing through a conductor the current density decreases exponentially from the surface towards the centre of the conductor. Thus, the skin depth, $\delta_{m,}$ is defined as the depth where the current is 1/e of the value of the surface. It can be expressed as shown in equation 2. The value of the skin depth is affected by μ. When an external magnetic field is

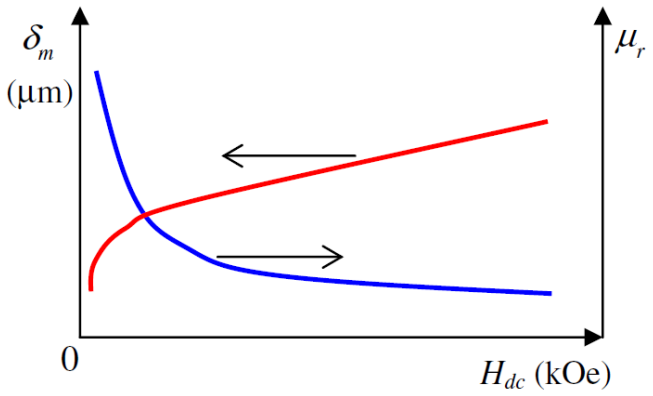

Figure 3 Skin Depth, δ_m (red) and relative permeability, μ_r (blue), as a function of an external magnetic field, H_{dc}, for a soft magnetic material.

applied to a conductor μ varies as a function of *Hdc* reaching at the saturation point the minimum value equal to μ_0 (see Figure 3).

Therefore, as equation 2 shows, a decrease in μ has associated an increase of the skin depth of the conductor ($\delta_{m,}$).

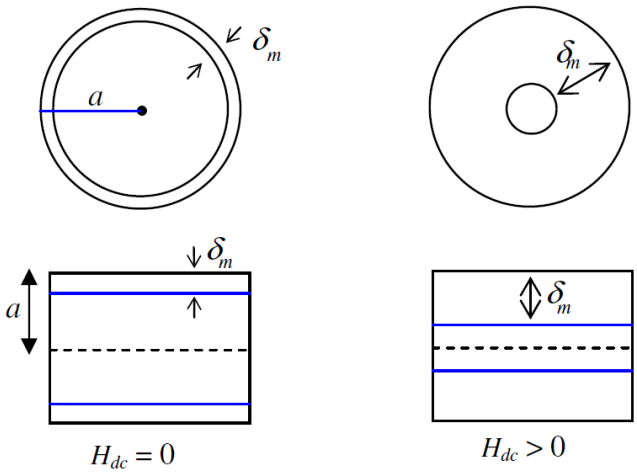

Figure 4 Skin depth of the conductor as a function of the magnetic field applied to it.

As a result of the increase of δ_m, the current will flow through a larger effective cross sectional area, giving rise to a decrease in the electric impedance of the magnetic conductor, *Z*, with the magnetic field (Z (H_{dc} = 0) > Z (H_{dc} >0)). This is the basis of the position sensor for detecting vibration. The operation principle relies on the variation of the impedance of the sensor nucleus under the action of the magnetic field generated by a small magnet attached to the vibrating element.

The intensity of a magnetic field created by a permanent magnet (H_m) could be approximated to be inverse related to the cube of the distance to a point, therefore variations in the position of the magnet to respect to a sensor will produce changes in the magnetic field acting on sensor. These changes in the magnetic field will produce changes in the skin depth of the sample producing a variation in the impedance.

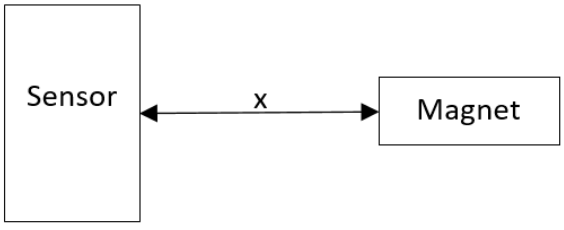

Figure 5 Schematic of the utility of the sensor.

In industrial applications machines usually have a low frequency vibration in the range of 5-50 Hz. Employing a magnet attached to a vibrating machine, the vibration will produce a variation of the magnetic field at the sensor position that can be detected through changes in *Z*.

Objectives

The objective of this work is to design a sensor capable of measuring vibrations in a certain domain of low frequencies.

First of all, the material employed in sensor nucleus should be selected and characterized as a function of frequency and amplitude of the exciting current, in order to achieve maximum changes in the impedance.

Once the material of the *GMI* sensor was optimized, the magnetic field generated by the permanent magnet that will be attached to the vibrating object should be characterized. The optimum distance magnet-sensor should be determined to achieve maximum sensor sensitivity.

Finally, the amplitude of the vibration of a moving object will be characterized with the help of an accelerometer and a shaker.

Methodology

In order to fulfil the objectives described before the first step was to characterize the different available samples. There were two different formats, the ribbon and the wire form. These samples were obtained by rapid-quenching of the melt (melt-spinning technique for the ribbon and in-rotating-water quenching technique for the wire). The rapid solidification procedure leads in both cases to an amorphous structure characterized by a soft magnetic behaviour (high magnetic permeability and low coercive fields). [9]

The **ribbon** sample has the composition, $(\mathbf{Co_{0,014}\ Fe_{0,06}})_{72,25}\ \mathbf{Si_{12,5}\ B_{15}}$, and will be mentioned from now on as **ribbon**.

The **wire** sample has the composition, $\mathbf{Co_{66}Fe_2Si_{13}B_{15}Cr_4}$, and will be mentioned from now on as **wire**.

By means of the characterization of the samples it will be possible to select the sensor nucleus with optimum response (maximum GMI ratio). (see equation 1)

Once the factors related with the sample were determined, it was necessary to evaluate the optimal position of the sample with respect to the magnet that generates the magnetic field. Thus, in order to obtain correct results, it was necessary to previously characterize the magnetic field generated by the magnet.

After the selection of the sample and the determination of the optimal distance, it was possible to study the vibrations conditions in which the sensor could work.

Characterization of the samples as a function of the frequency and amplitude of the electric current

The first step in this work consisted on acquiring the ability to work with the samples. It was necessary to weld the samples to the circuit (see Figure 6) in order to measure the voltage and current on them. Then, each sample was characterized as a function of the frequency and the amplitude of the electric current flowing through it.

The circuit in figure 6 consisted on a voltage divider with a resistor R = 20 Ω and the impedance of the sensor in series. A function generator GW Instek AFG 2005 was employed to provide the *ac* current (V_{in}). The voltage drop V_{ac} of the sensor was characterized through an oscilloscope Tektronix TDS 3012B.

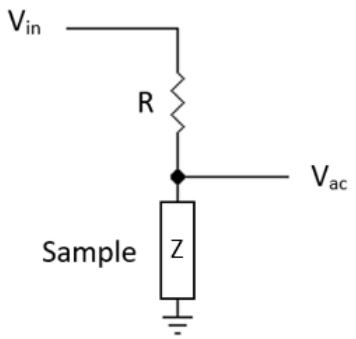

Figure 6 Schematic of the circuit used in the characterization of the samples.

The current was measured through an AC current sensor clamp (Tektronix P6022) at any point of the circuit shown in Figure 6. It was very relevant to keep intensity current constant during characterization as the impedance of the sample was varying in order to obtain proper measures.

In order to characterize the samples, a frequency sweep was made with a step of 50 kHz. For each value of the frequency, under a constant value of the amplitude of the current, the impedance of the sample (*Z=Vac/Iac*) was measured at null and at saturation magnetic field. Following equation 1 the values of the relative variation of the impedance for each frequency were obtained.

Once the optimal frequency was found (ΔZ/Z maximum), a swept in current was performed with intervals of 0.5 mA at null H_{dc} in order to find the value that optimizes the effect. This H_{dc} was generated employing a homemade solenoid which its characterization curve is shown below.

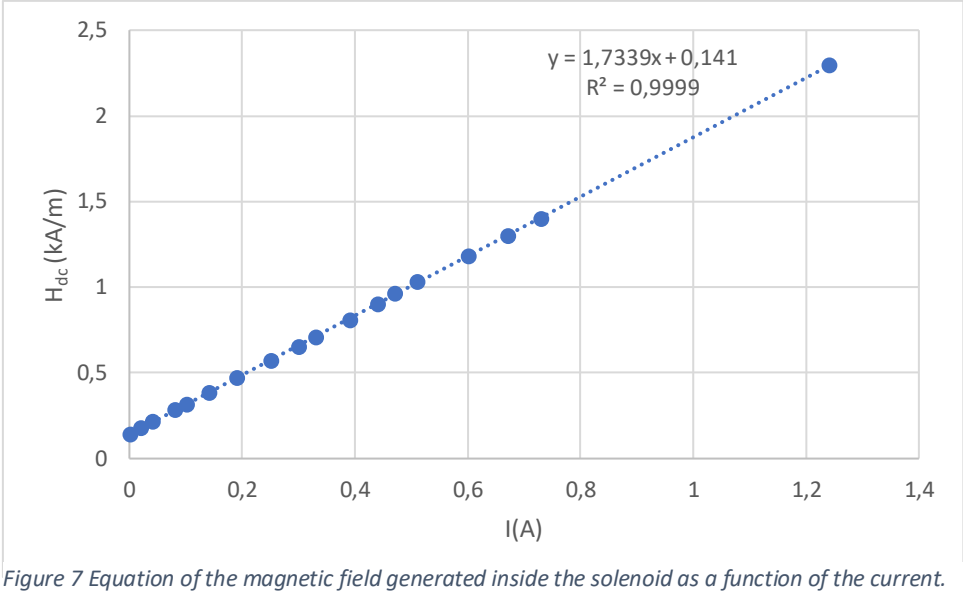

Figure 7 Equation of the magnetic field generated inside the solenoid as a function of the current.

Characterization of the samples under a static magnetic field

In our sensor prototype a magnet is employed to generate the magnetic field, H_m. Unlike a solenoid, the magnetic field of a magnet is not homogeneous. So, it was needed to study the intensity of the magnetic field generated for each side of the magnet in order to optimize subsequent variations in *Z*.

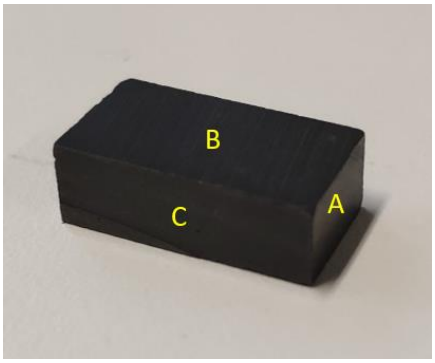

Figure 8 Faces of the magnet.

With a LakeShore 475 DSP Gaussmeter, the magnetic field produced by the magnet was measured as a function of the distance for different faces shown in Figure 8.

Face B of the magnet is the side which produces the maximum intensity on its surface so it will be used in the following steps. The data are presented on Figure 9.

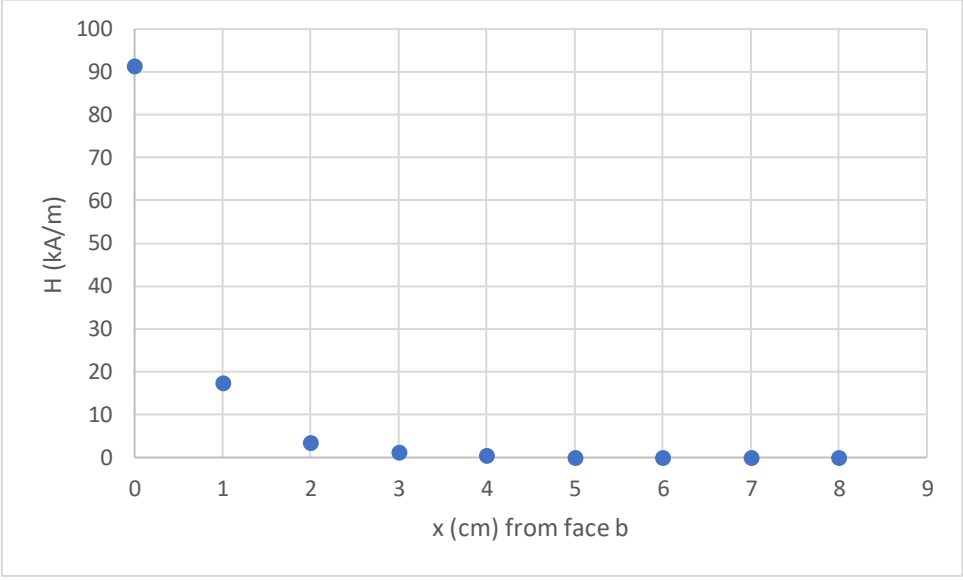

Figure 9 Magnetic field generated by the magnet as a function of the distance to the surface.

Variation of the voltage of the sample with the distance to the magnet

Before characterizing the vibration amplitude, it was needed to determine the optimum distance (*x*) at which the sensor shows the largest differences in voltage, what is the same, it

was needed to obtain which sample had the highest sensitivity and at which range. (see Figure 10)

For that purpose, the magnet was fixed to a micrometer screw (see Figure 11) capable of moving it forward and backwards with precision of 0.002 cm. In front of it we put the sample welded to the contacts which were attached to a plastic flat surface through epoxy araldite in order to give our sample a more solid base. (see Figure 12)

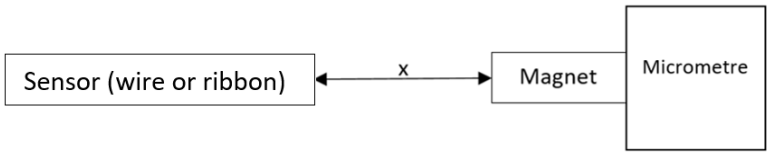

Figure 11 Scheme of the magnet and the sensor in this phase of the work.

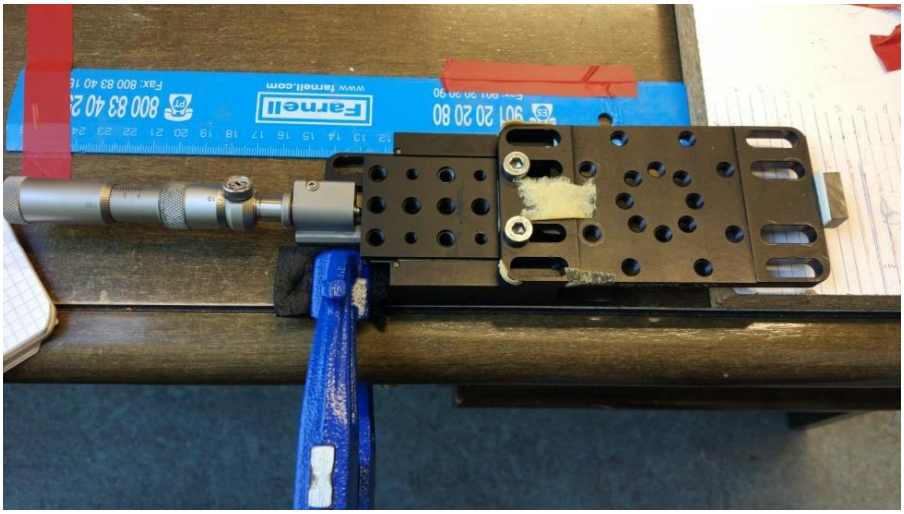

Figure 10 Micrometre with magnet attached to its end.

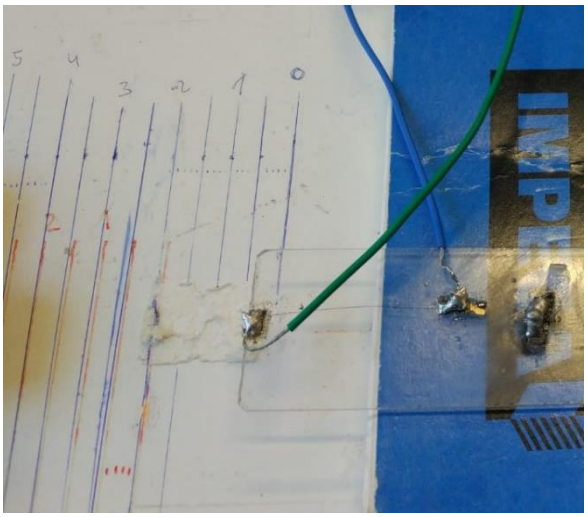

Figure 12 Sample located with the scale in order to move the magnet every 0.5 cm.

With the material fixed to the working place in order to obtain precise results without moving anything by mistake, and moving the magnet away from the sensor with the micrometer screw, the sensor response was characterized firstly every 0.5 cm in order to narrow down the length of the study. After that, the process was repeated every 0.1 cm and then every 0.002 cm taking note of the values of the voltage, V_{ac}, that were measured by a Hewlett Packard 34401A. The sample was excited by a Stanford Research Systems DS345 Synthesized Function Generator with a sinusoidal signal, employing optimal values of frequency and amplitude of the current.

As we move the magnet with the micrometer a distance, x, the voltage is measured with the multimeter. This way we can calculate the variation in each interval and choose the one with the greatest variation, this is the one in which the sample has the biggest sensitivity. For the next step this range would be the ideal zone to work with as the variations of the impedance of the sample will be maximum.

Once that the optimum distance range was characterized, the sensor response was characterized (V_{ac} versus x) in the micrometric range with the help of the micrometer screw. For the next step, the range leading to the maximum impedance variation will be selected.

Characterization of the selected sample under a vibrating magnetic field

Once the sensitivity of the sample was calculated the next step was to recreate a setting as similar to the real purpose of the sensor as possible, capable of measuring the amplitude of the vibrations. To simulate those conditions a shaker (LDS V201) was employed. It was excited by a Sony Tektronix AFG 310 to supply an oscillation of low frequency (typical of industrial machinery). As can be seen in Figure 13 the magnet was placed on the top and the sensor at the optimal distance, changing its impedance as a result of the vibration of the magnet which described a simple harmonic motion. The sensor was fixed to the ground, remaining at rest.

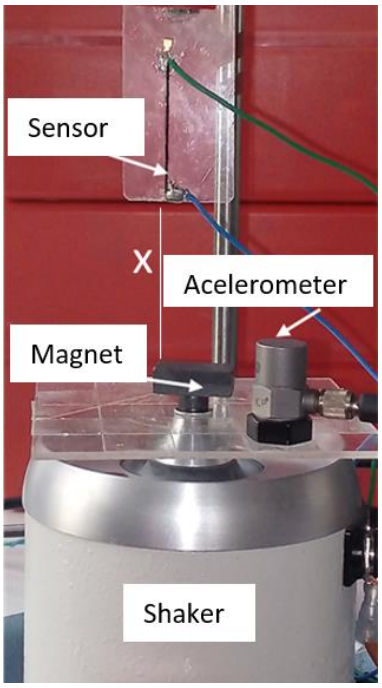

Figure 13 Setting of the shaker with the magnet and the sensor.

Then, the shaker will make the magnet move with a simple harmonic motion with respect to the sensor, being the position of the magnet given by:

$$x(t) = A\,cos(wt + \varphi) \qquad (3)$$

Being *A* the amplitude of the oscillation, $w=2\pi f$, angular frequency of the oscillation and φ the phase. Making the second derivative it was obtained the value of the acceleration for each moment of the movement.

$$a(t) = -Aw^2\cos(\mathrm{wt} + \varphi) \qquad (4)$$

Simultaneously an accelerometer (PCD 352C33) was employed to characterize the vibration acceleration (a) (100 mV per 9.8 m/s^2). Thus, the value the amplitude of the movement could be obtained by the following expression from experimental parameters:

$$A = \left|\frac{a_{max}}{w^2}\right| \qquad (5)$$

With a function generator GFG-8216 the amplitude of the current and the frequency of the exciting current of the GMI sensor were fixed at the optimal values of **400 kHz** and **19.6 mA**.

Since for a potential final device, a triangular signal is easier to generate than a sinusoidal one, the sensor response was analysed under both types of signal.

As a result of the vibration, the changes on sensor impedance (due to changes on H_m acting on sensor) leaded to an AM modulated signal where the amplitude of modulated signal (V_{env+} or V_{env-}) was proportional to A (see Figure 15). The minimum on V_{env+} or V_{env-} represents the moment in which the distance between magnet and sensor is minimum, while the maximum of the same signal will represent the maximum distance.

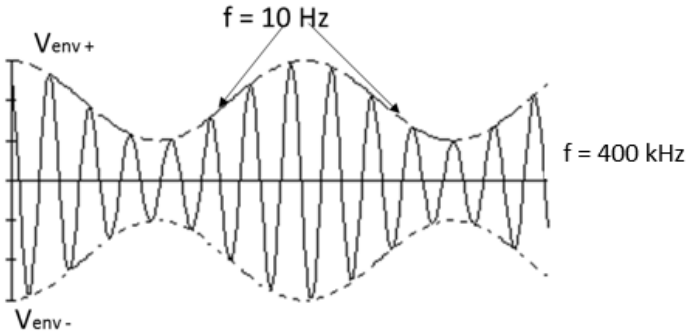

Figure 14 Representation of the AM modulated signal obtained during vibration, 400 kHz, and the signal obtained in the second phase ("Detectores envolvente positivo y negativo") of the electronic interface of Figure 15 ***¡Error! No se encuentra el origen de la referencia.****, 10 Hz.*

In order to determine Venv+ (or Venv-) an electronic interface was designed (in collaboration with the department of "Ingenieria Eléctrica, Electrónica y de Comunicación de la UPNA") based on AM demodulation.

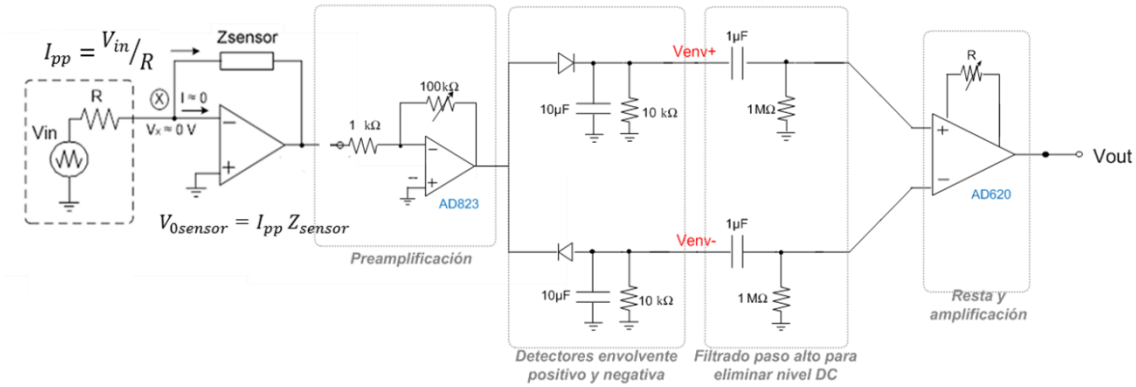

Figure 15 Schematic of the electronic interface necessary to obtain a value of the amplitude of the vibration as a function of the variation of the impedance of the sample.

The electric interface was supplied by ±5 V source and it was formed by an initial stage of sensor excitation, a second stage of demodulation.

The initial stage was supplied by a triangular and a sinusoidal signal as it was commented before by a function generator (Standford Research Systems DS 345, V_{in}) in series with a resistor, R, obtaining a current, $I_{pp} = V_{in}/R$. Those values of R and V_{in} were selected in order to work with the optimal frequencies of the sensor. The sensor is located in the negative closed loop. The positive terminal is connected to ground fixing the potential of the negative terminal to that same value. This way it is assured that I_{pp} will flow with a constant value through the sensor all the time,

obtaining at the end of the amplifier a signal $V_{0sensor}=I_{pp} * Z_{sensor}$, which depends lineally on the variation of the impedance of the sensor as it was desired.

After that first phase the next step was to amplify that signal increasing the amplitude of the enveloping signal. That signal then was demodulated. In a first substage enveloping detectors (diodes) were used to estimate the difference between the maximum and minimum values of V_{env+} and V_{env-}. Then a high-pass filter was used to eliminate the DC component of enveloping signals.

The last stage subtracts and amplifies the AC component of the enveloping signals obtaining the final signal $\boldsymbol{V_{out}}$ that was measured by a Tektronix MDO3024 Mixed Domain Oscilloscope. In this same oscilloscope thanks to PCB 480C02 ICB sensor signal conditioner it was represented the signal measured by the PCD 352C33 **accelerometer** fixed to the shaker.

Measuring the Peak to Peak value of both the accelerometer and the conditioned sensor signal, the response of the sensor to the movement of the magnet attached to the shaker for the different frequencies between **5 and 50 Hz** every **5 Hz** was characterized.

Results and analysis of the work.

First phase: Selection of the sample

In this first phase the objective was to choose the optimum sample between the ribbon and the wire of 3 cm in length each. For that reason, it was needed to characterize the behaviour of the different samples and compare their response. The main characteristic that will be taken into account will be the sensitivity of the different materials.

Characterization of the wire in frequency and amplitude of the current

The first step was to characterize the wire, as indicated in the section Characterization of the samples as a function of the frequency and amplitude of the electric current.

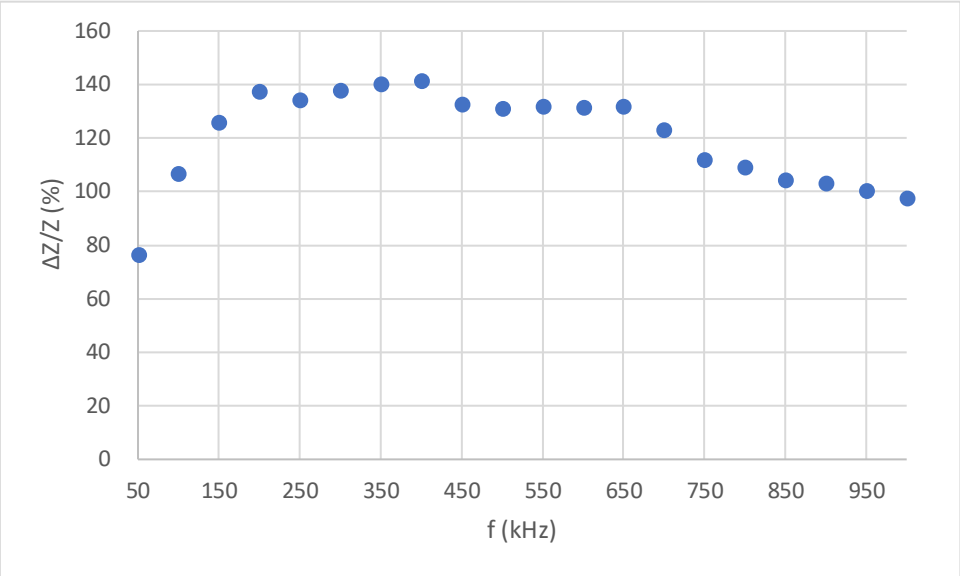

Figure 16 Relative variation of the impedance of a 3 cm wire, Δz/z, as a function of the frequency, f, for a current of 10 mA.

The optimal frequency obtained was of **400 kHz**, which is the value used to obtain the optimal current and the one that will be used from now on when working with samples of wire.

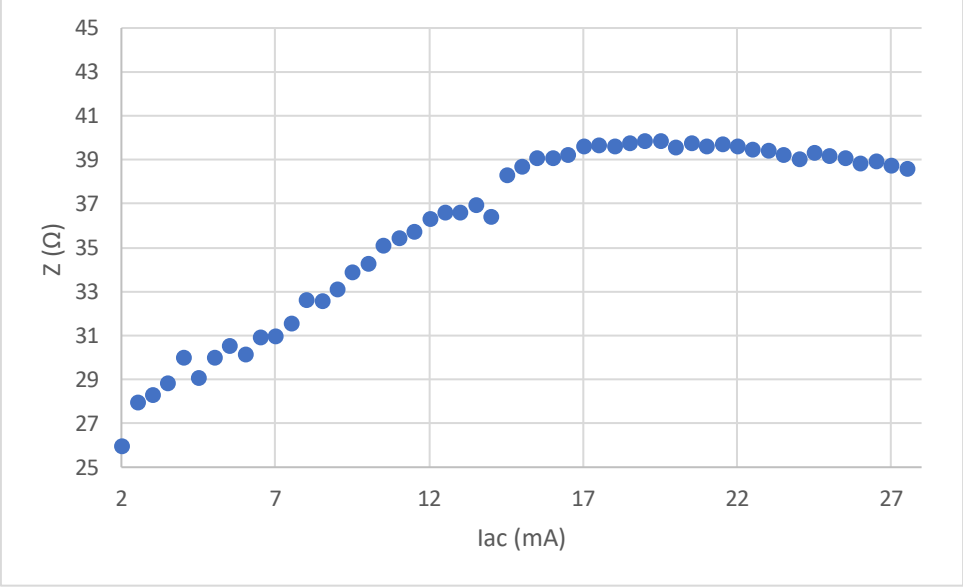

Figure 17 Impedance of the wire, Z, as a function of the current supplied to it, Iac, for a frequency of 400 kHz.

As it can be seen in Figure 17 the optimal value for the current in the wire is of 19.5 mA, which will be used from now on for the wire. So, the optimal values will be a frequency of **400 kHz** and a current of **19.5 mA**. With that values in mind, next step was to calculate the impedance as a function of the magnetic field.

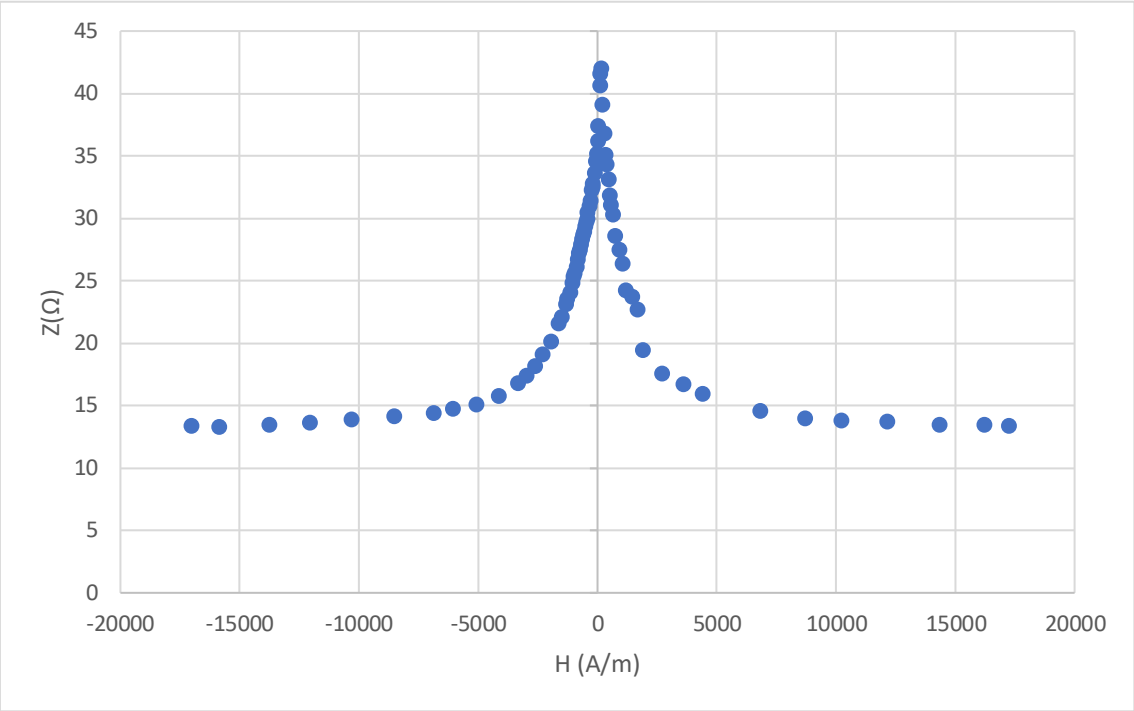

Figure 18 Impedance of the sample, Z, as a function of the magnetic field, H, for a sample of wire of 3 cm.

Characterization of the ribbon in frequency and amplitude of the current

After having studied the behaviour of the wire, it is turn to test the ribbon in order to compare between the two of them. In this case the sample used is a ribbon of 3 cm.

The first study was to calculate the optimal frequency and current for this new sample.

In this case the optimal frequency was obtained at **200 kHz**, which is the value used to obtain the optimal current (see Figure 20) and the one that will be used when working with samples of the ribbon.

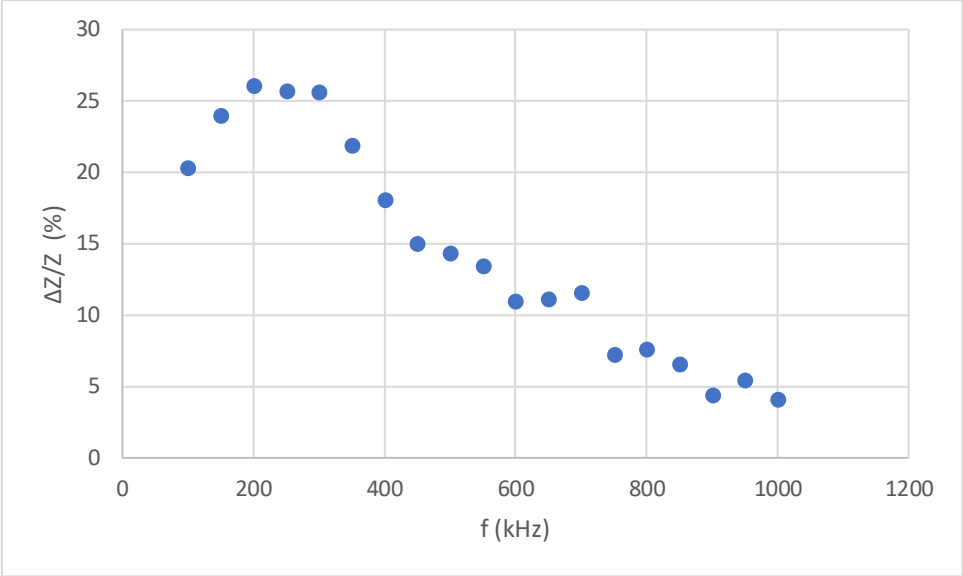

Figure 19 Relative variation of the impedance of a ribbon of 3 cm, Δz/z, as a function of the frequency, f, for a current of 10 mA.

Then the value of optimal current amplitude was analysed:

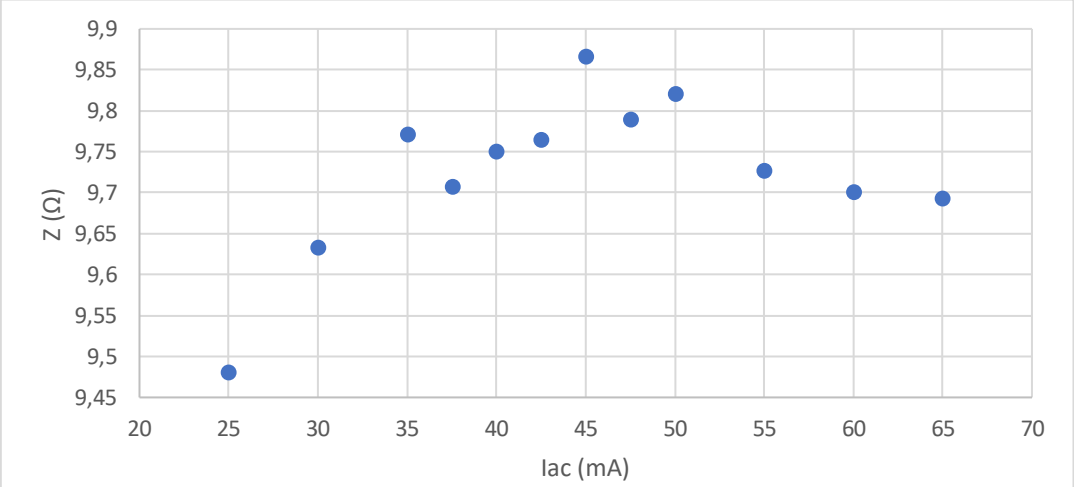

Figure 20 Impedance of the ribbon of 3 cm, Z, as a function of the current supplied to it, Iac, for a frequency of 200 kHz.

Optimal values for the ribbon were obtained for frequency and current of **200 kHz** and **45 mA**. In Figure 21 is shown the impedance as a function of the magnetic field for our sample.

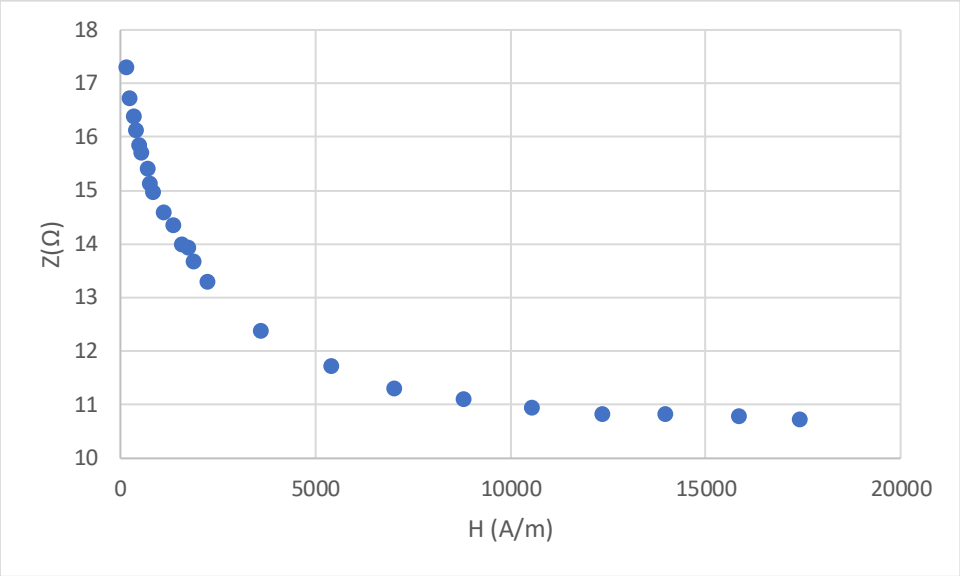

Figure 21 Impedance of the sample, Z, as a function of the magnetic field, H, for a sample of ribbon.

Employing equation 1 it can be seen that the wire displays a maximum impedance variation $\Delta Z/Z$ around, 140%, in comparison with the ribbon around, 25%, for a length of 3 cm.

Variation of the voltage of the wire of 3 cm with the distance to the magnet

The next step was to characterize the impedance voltage as a function of the distance, *x*, between the magnet and the sensor. First it was made with the wire of 3 cm.

Firstly, the variation of the voltage of the sample as a function of the magnet position (each 0.5 cm) was determined (see Figure 22).

In this case the maximum sensitivity is obtained in the range between **0.5** and 2 **cm** with a maximum value of **33.4 mV/cm**.

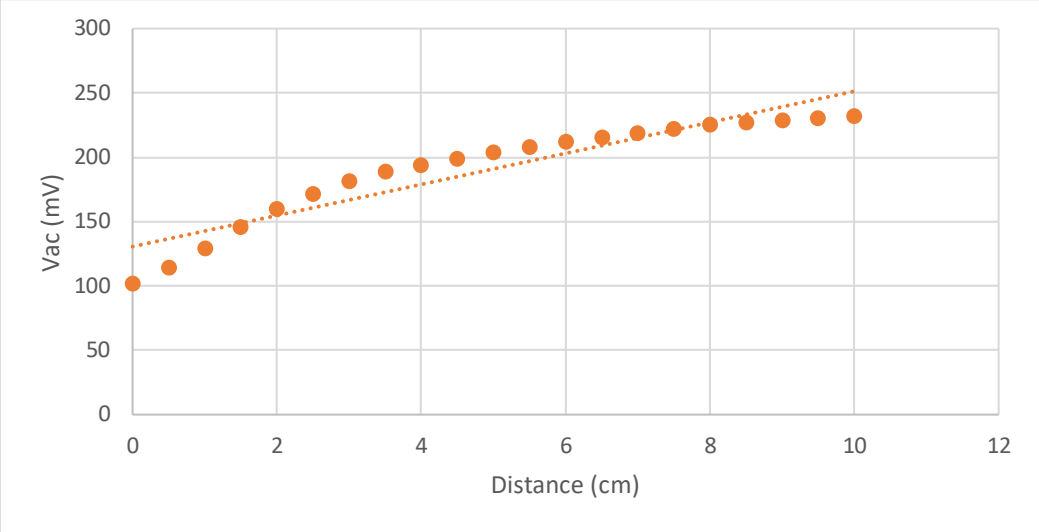

Figure 22 Voltage of the wire of 3 cm, Vac, as a function of the magnet distance (step 0.5 cm).

Therefore, the next study was carried for that range, taking this time measures every 0.1 cm.

In this new study it was obtained a set of points with a mean slope considering the whole interval of around **30.5 mV/cm**. (see Figure 23) The maximum variation between two consecutive points was located between 1.4 and 1.5 cm with a maximum value of the slope of 36.7 mV/cm as it can be seen in the next figure.

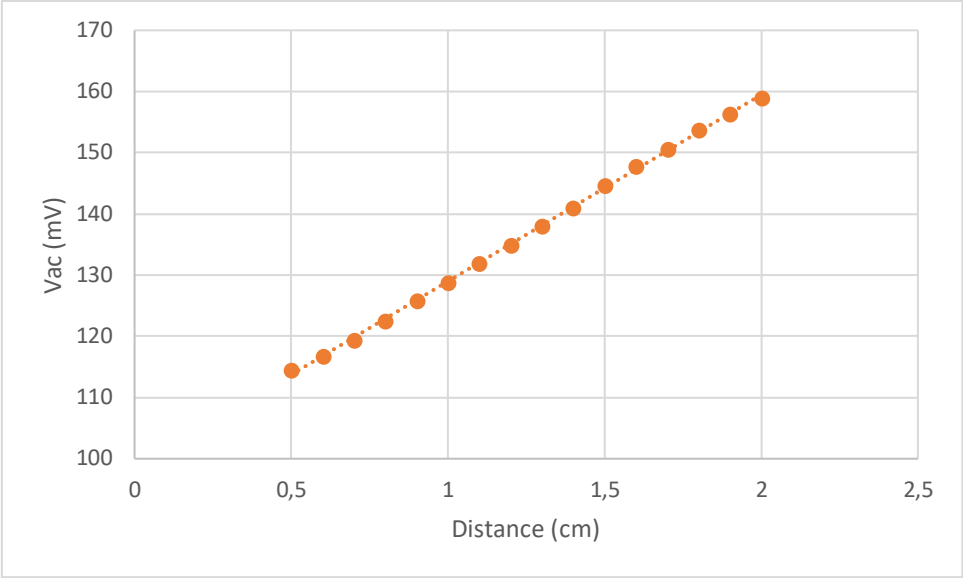

Figure 23 Voltage of the wire of 3 cm, Vac, as a function of the magnet distance (step 0.1 cm).

Thus, the micrometric study was carried out in the region between 1.4 and 1.5 cm.

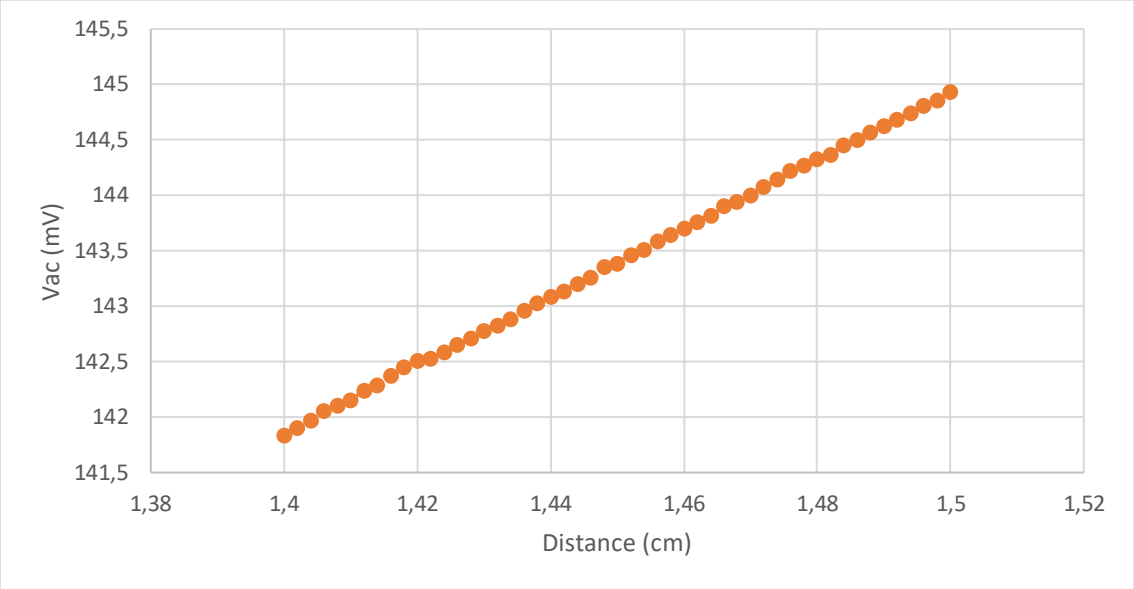

Figure 24 Voltage of the wire of 3 cm, Vac, as a function of the magnet distance (step 0.002 cm).

In Figure 24 it can be observed the linear response of the sensor in the micrometric range. The mean slope of the region is around **30.8mV/cm** as expected from the study of the millimetres. Then, it can be concluded that the maximum sensitivity of the wire is located in the interval between 1.4 and 1.5 with a value of around 30.8 mV/cm.

Variation of the voltage of the ribbon of 3 cm with the distance to the magnet

Analogously, the study of the variation of the voltage for the ribbon of 3 cm was started with a 0.5 cm step.

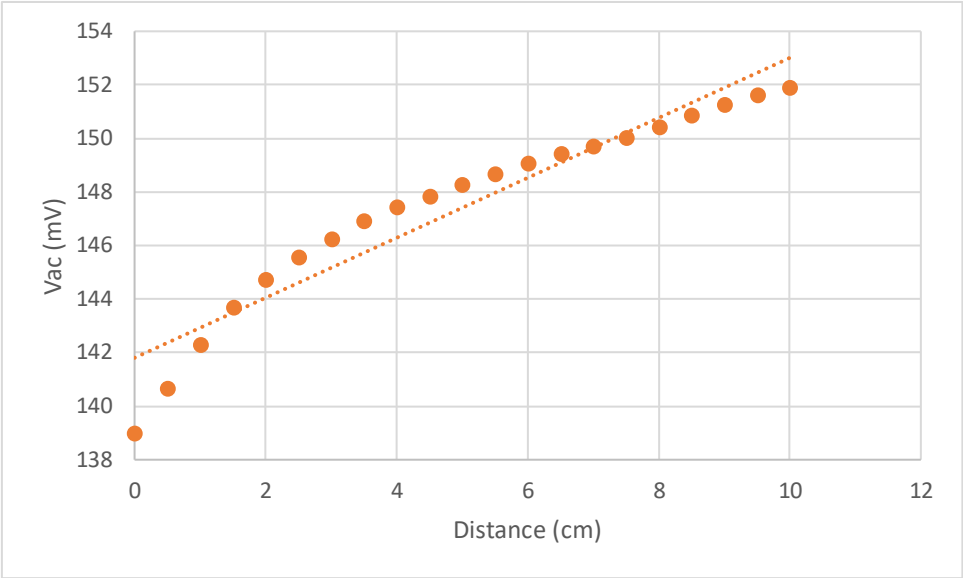

Figure 25 Voltage of the sample of 3 cm, Vac, as a function of the magnet distance (step 0.5 cm).

In this case the maximum slope value was 3**.4mV/cm** in the range between **0** and **2 cm,** being this the range that will be analysed next.

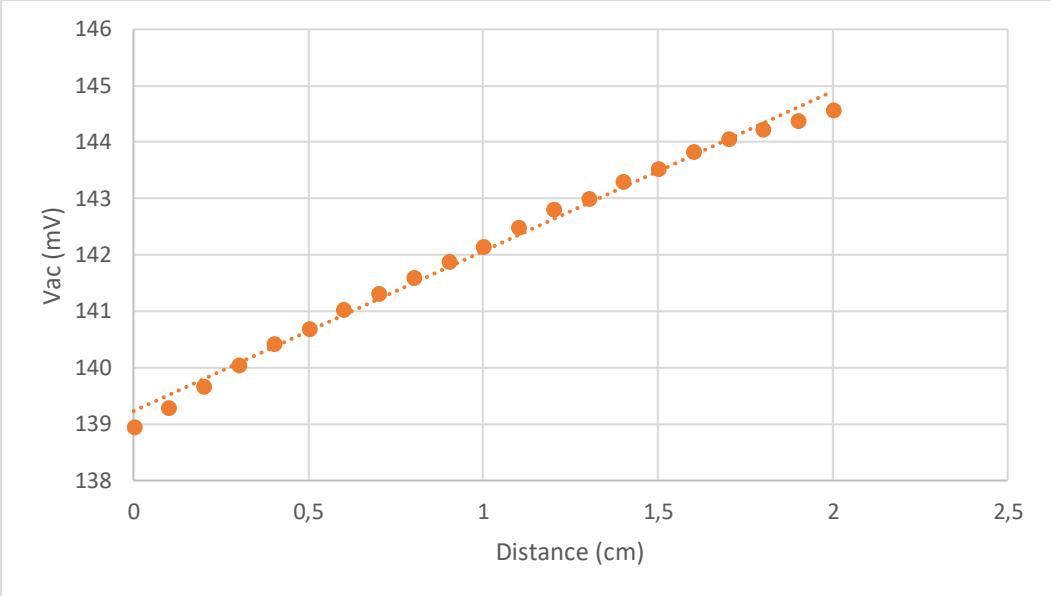

Figure 26 Voltage of the sample of 3 cm, Vac, as a function of the magnet distance (step 0.1 cm).

In this range the maximum slope between consecutive points was achieved at the range between 0.2 and 0.3 cm with a value of **3.7 mV/cm.**

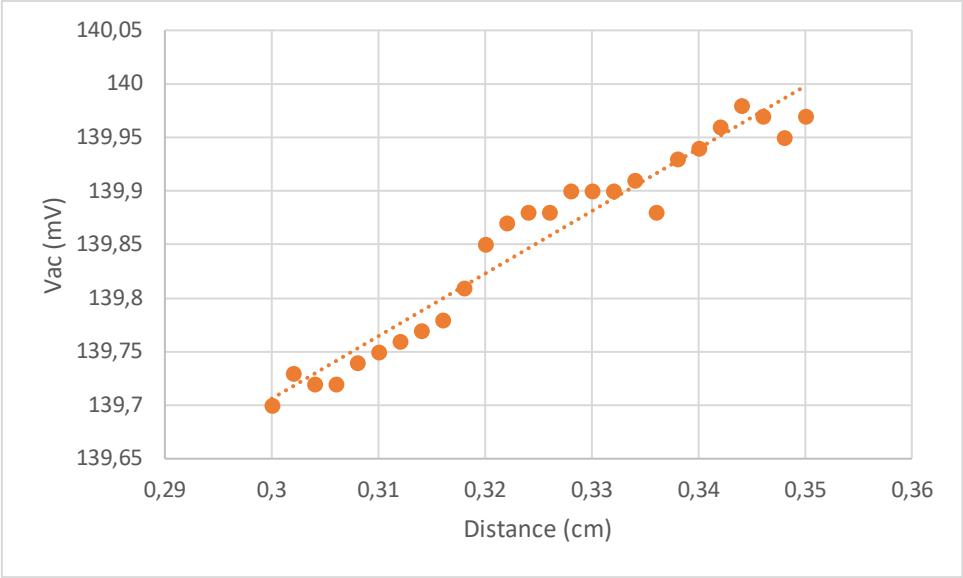

Figure 27 Voltage of the sample of 3 cm, Vac, as a function of the magnet distance (step 0.002 cm).

In this last study, Figure 27, the low voltage variations led to a certain error in the measurements. Nonetheless, it can be seen how the tendency is lineal, with a value of the slope of about **5.8 mV/cm**. This will be the micrometric sensitivity of the sample.

Looking at the values of the sensitivity obtained for the ribbon and wire with values of 5.8 mV/cm and 30.8 mV/cm respectively it can be concluded that the sensitivity of the sample wire is higher, **5.6 times higher**. These results confirm the previous conditions when both samples were submitted to a homogeneous dc magnetic field. That is, the wire sample displays the highest sensitivity under magnetic field variations.

As the GMI ratio depends on the sample length, L, the dependence of ΔZ/Z (%) on L was analyzed in the ribbon to check whether the variation on length could fill the gap between the ribbon and the wire.

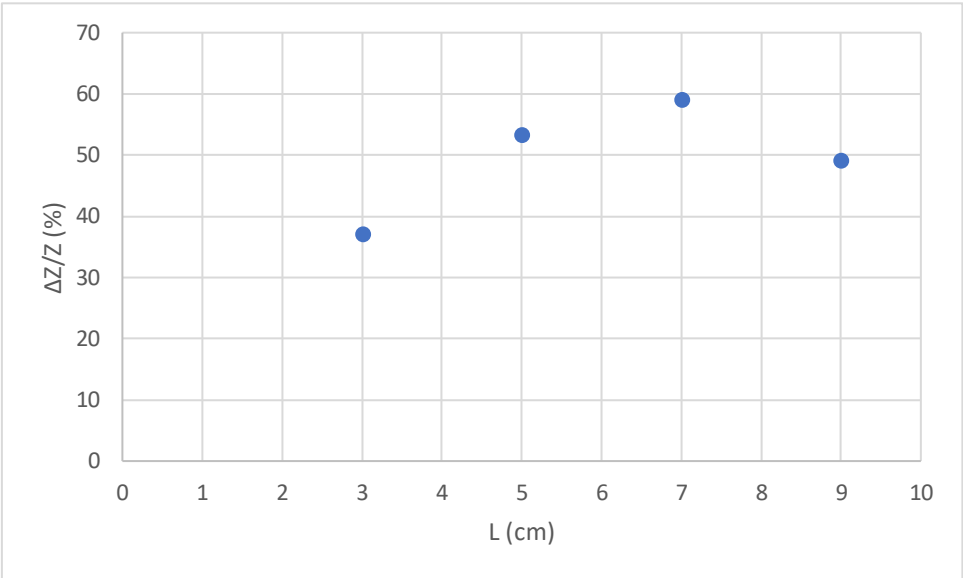

Figure 28 Variation of the impedance for different lengths of the ribbon of ribbon with the optimal values of frequency and current of 200 kHz and 45 mA.

As it can be seen in Figure 28 the maximum variation of the impedance for a sample of ribbon varies with the length and has its maximum value for a length of 7 cm. Therefore, it will be studied the variation of the voltage of the ribbon with the distance to the magnet for a sample of 7 cm. In order to compare the results.

Variation of the voltage of the ribbon of 7 cm with the distance to the magnet

The same procedure followed in the two other cases is carried out for this new sample of ribbon.

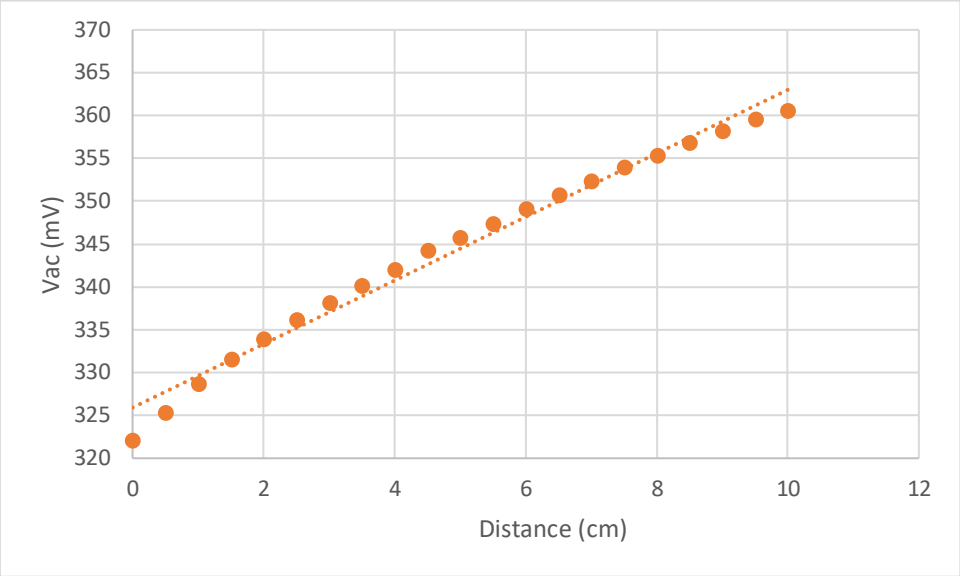

Figure 29 Voltage of the sample of 7 cm, Vac, as a function of the magnet distance (step 0.5 cm).

From Figure 29**¡Error! No se encuentra el origen de la referencia.** data, the range between **0** and **2 cm** exhibits the maximum sensitivity with a value of with a maximum value of **6.68 mV/cm**.

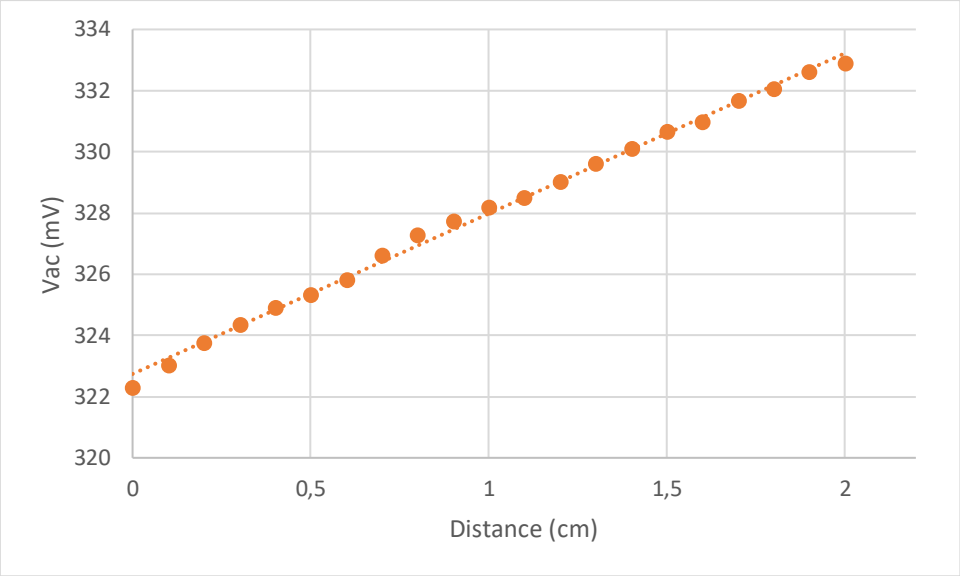

Figure 30 Voltage of the sample of 7 cm, Vac, as a function of the magnet distance (step 0.1 cm).

The next study was made in that range of 2 cm. Taking this time measures every 0.1 cm. In this case the maximum slope is produced between **0.6** and **0.7 cm** with a value of maximum sensitivity for this second study of **7.7 mV/cm**. In that range the last study each 0.01 cm was performed. Data are represented in Figure 31.

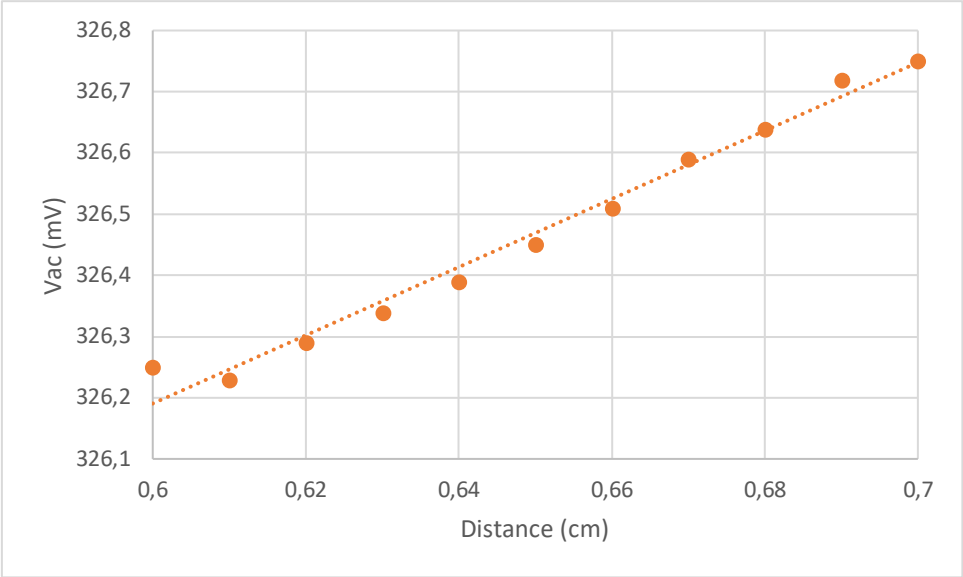

Figure 31 Voltage of the sample of 7 cm, Vac, when moving the magnet away from it, every 0.01 cm.

The linear tendency of the three previous graphs maintains a slope of about 5.5 mV/cm in the region of maximum variation, so this could be approximately considered as the correct sensitivity of the sample.

Conclusions of the first phase

Even though a higher GMI ratio was found for L=7 cm for the ribbon it is below the obtained value for the wire. It can be concluded that the **sensitivity** of the **wire** is really **5.6 time higher**.

Therefore, the **sample used** in the second phase of the work will be with a **wire** of **3 cm** located around **1.5 cm away from the magnet** and with optimal values of frequency and current of **400 kHz** and **19.5 mA**.

Second phase: Characterization of the shaker with the magnet.

Once the arrangement explained in "Characterization of the selected sample under a vibrating magnetic field" was performed, it was proceeded to make the swept in frequencies in order to study the response of the sensor to those different vibrations. The results obtained are the following.

In this step, it was measured the voltage of the sensor (V_{out}) and the voltage given by the accelerometer as the magnet was vibrating along with the shaker with different amplitudes (A). The signal given by the accelerometer (mV) was converted into an amplitude of the vibration (mm) as explained in Characterization of the selected sample under a vibrating magnetic field (see Equation 5).

Vibration of 5 Hz

Senoidal		Triangular	
Vout (mV)	Vibration Amplitude (mm)	Vout (mV)	Vibration Amplitude (mm)
672	0.010	640	0.009
1060	0.014	760	0.010
1260	0.016	840	0.011
1540	0.020	960	0.012
1720	0.022	1080	0.014
-	-	1160	0.015
-	-	1280	0.017

Figure 32 Values of the voltage of the sensor and the amplitude of vibration for a sinusoidal and a triangular signal with frequency of 5 Hz.

Vibration of 10 Hz

Senoidal		Triangular	
Vout (mV)	Vibration Amplitude (mm)	Vout (mV)	Vibration Amplitude (mm)
536	0.007	528	0.007
616	0.006	668	0.009
712	0.010	696	0.010
800	0.011	784	0.011
888	0.013	880	0.013
976	0.014	952	0.014
1060	0.015	1060	0.016

Figure 33 Values of the voltage of the sensor and the amplitude of vibration for a sinusoidal and a triangular signal with frequency of 10 Hz.

Vibration of 15 Hz

Senoidal		Triangular	
Vout (mV)	Vibration Amplitude (mm)	Vout (mV)	Vibration Amplitude (mm)
464	0.008	452	0.008
544	0.009	536	0.009
624	0.011	604	0.011
712	0.012	680	0.012
776	0.014	768	0.014
856	0.016	840	0.016
936	0.018	912	0.018

Figure 34 Values of the voltage of the sensor and the amplitude of vibration for a sinusoidal and a triangular signal with frequency of 15 Hz.

Vibration of 20 Hz

Senoidal		Triangular	
Vout (mV)	Vibration Amplitude (mm)	Vout (mV)	Vibration Amplitude (mm)
440	0.009	432	0.009
520	0.011	512	0.011
592	0.013	584	0.012
664	0.014	656	0.014
728	0.016	728	0.016
808	0.018	792	0.018
880	0.020	872	0.020

Figure 35 Values of the voltage of the sensor and the amplitude of vibration for a sinusoidal and a triangular signal with frequency of 20 Hz.

Vibration of 25 Hz

Senoidal		Triangular	
Vout (mV)	Vibration Amplitude (mm)	Vout (mV)	Vibration Amplitude (mm)
432	0.011	440	0.012
508	0.013	504	0.014
592	0.016	584	0.016
664	0.018	648	0.019
736	0.020	720	0.021
816	0.023	800	0.023
896	0.025	872	0.025

Figure 36 Values of the voltage of the sensor and the amplitude of vibration for a sinusoidal and a triangular signal with frequency of 25 Hz.

Vibration of 30 Hz

Senoidal		Triangular	
Vout (mV)	Vibration Amplitude (mm)	Vout (mV)	Vibration Amplitude (mm)
509	0.014	504	0.015
596	0.017	584	0.017
672	0.019	672	0.020
760	0.022	752	0.023
848	0.025	840	0.025
920	0.028	896	0.028
1000	0.030	984	0.030

Figure 37 Values of the voltage of the sensor and the amplitude of vibration for a sinusoidal and a triangular signal with frequency of 30 Hz.

Vibration of 35 Hz

Senoidal		Triangular	
Vout (mV)	Vibration Amplitude (mm)	Vout (mV)	Vibration Amplitude (mm)
640	0.022	680	0.024
740	0.025	760	0.026
880	0.029	840	0.030
960	0.033	960	0.033
1080	0.036	1040	0.036
1120	0.039	1100	0.039
1200	0.042	1200	0.042

Figure 38 Values of the voltage of the sensor and the amplitude of vibration for a sinusoidal and a triangular signal with frequency of 35 Hz.

Vibration of 40 Hz

Senoidal		Triangular	
Vout (mV)	Vibration Amplitude (mm)	Vout (mV)	Vibration Amplitude (mm)
300	0.010	300	0.010
420	0.015	420	0.015
540	0.020	540	0.019
660	0.024	620	0.024
760	0.028	720	0.028
880	0.033	860	0.033
980	0.037	940	0.036
1040	0.040	1020	0.041
1160	0.044	1100	0.043
1240	0.047	1180	0.047
1280	0.051	1240	0.050

Figure 39 Values of the voltage of the sensor and the amplitude of vibration for a sinusoidal and a triangular signal with frequency of 40 Hz.

Vibration of 45 Hz

Senoidal		Triangular	
Vout (mV)	Vibration Amplitude (mm)	Vout (mV)	Vibration Amplitude (mm)
260	0.009	200	0.008
300	0.011	300	0.012
380	0.014	380	0.015
440	0.017	440	0.018
520	0.020	520	0.020
580	0.023	580	0.024
640	0.026	660	0.027
720	0.030	700	0.030
800	0.033	760	0.030
860	0.035	840	0.036
940	0.039	920	0.039

Figure 40 Values of the voltage of the sensor and the amplitude of vibration for a sinusoidal and a triangular signal with frequency of 45 Hz.

Vibration of 50 Hz

Senoidal		Triangular	
Vout (mV)	Vibration Amplitude (mm)	Vout (mV)	Vibration Amplitude (mm)
120	0.005	120	0.005
168	0.007	160	0.007
212	0.010	204	0.009
252	0.011	248	0.012
292	0.013	292	0.014
340	0.015	328	0.015
380	0.017	372	0.018
416	0.019	408	0.019
468	0.021	456	0.022
508	0.023	488	0.024
544	0.026	536	0.026

Figure 41 Values of the voltage of the sensor and the amplitude of vibration for a sinusoidal and a triangular signal with frequency of 50 Hz.

From the data of the tables it was represented V_{out} versus vibration amplitude in order to compare the results. Since the data are very similar between the sinusoidal and the triangular one, only the sinusoidal one was represented.

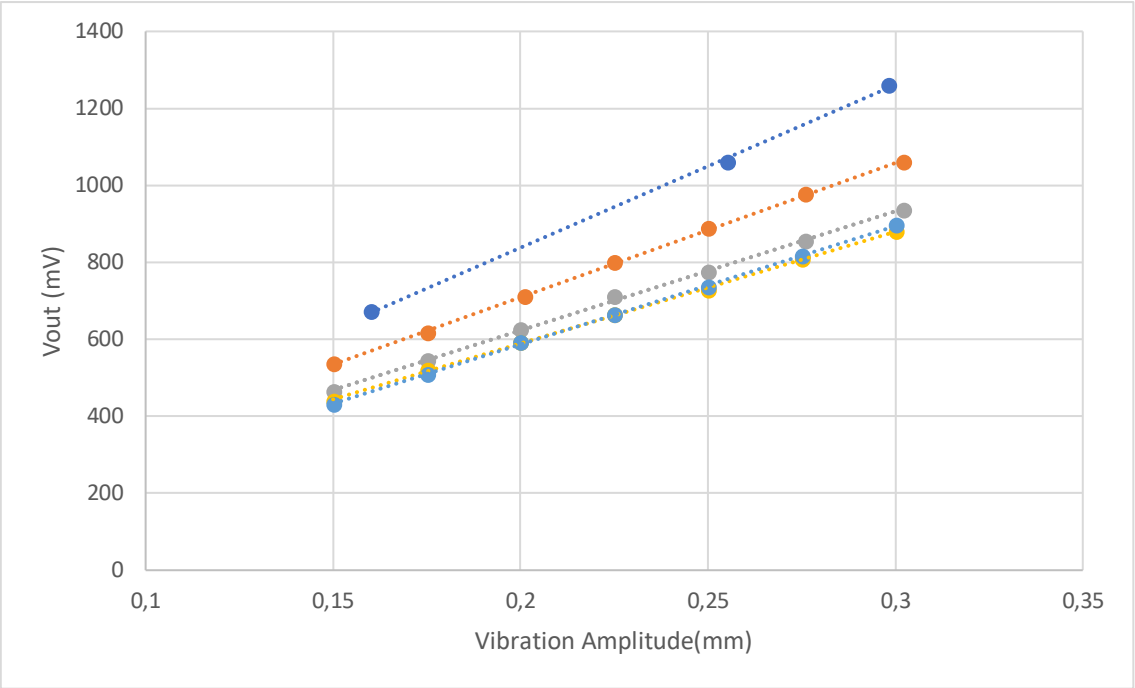

Figure 42 Results of the measurements of the sensor, Vout, as a function of the amplitude of the vibration (mm) for different frequencies from 5-25 Hz. 5 Hz (Blue), 10 Hz (Orange), 15 Hz (Grey), 20 Hz (Yellow) and 25 Hz (Cian).

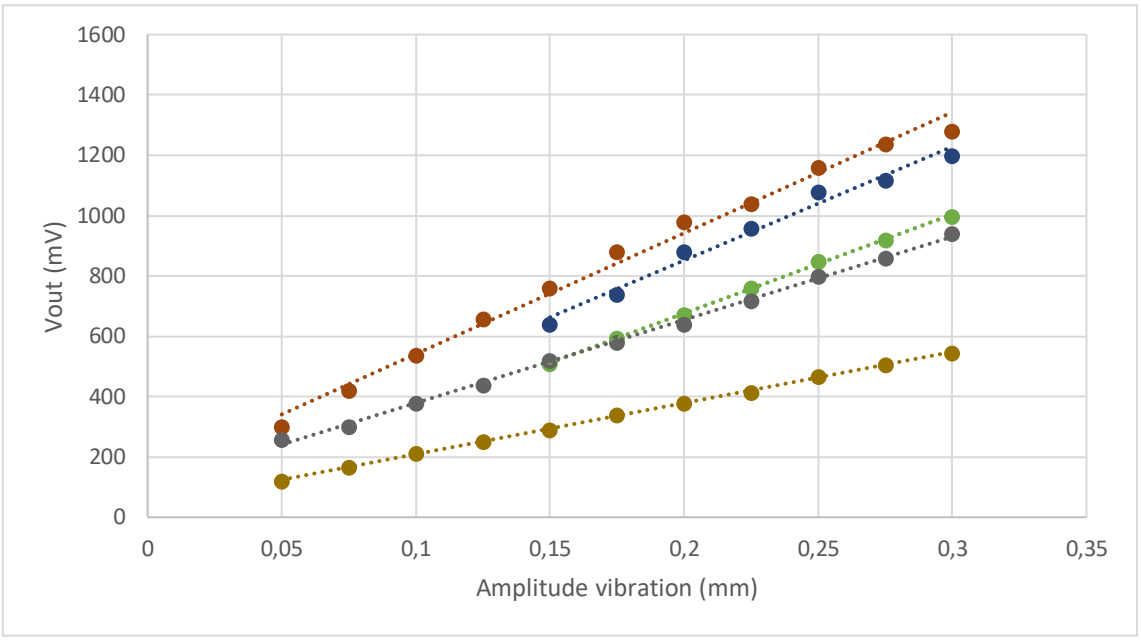

Figure 43 Results of the measurements of the sensor, Vout, as a function of the amplitude of the vibration (mm) for different frequencies from 30-50 Hz. 30 Hz (Green), 35 Hz (Dark blue), 40 Hz (Red), 45 Hz (Dark Grey) and 50 Hz

In Figure 42 and Figure 43 it can be observed how the voltage of the sensor (Vout) varies as a function of the amplitude of the vibration for the range of frequencies between 5 and 50 Hz.

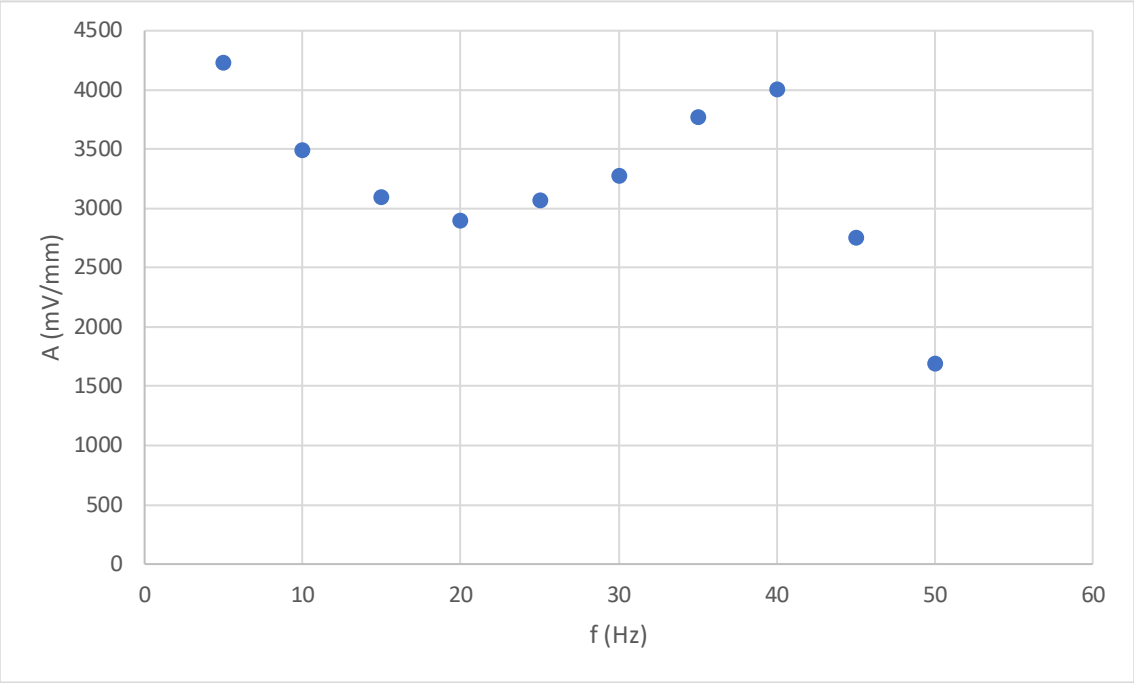

Figure 44 Sensitivity of the different lines of Figure 42 and Figure 43, A, for every different value of the frequency, f, from 5 Hz to 50 Hz, every 5 Hz.

It can be seen that the relation between the amplitude of the oscillation and the voltage of our sensor follows a straight line in all cases. It can also be observed that the triangular and sinusoidal signals give rise to a very similar response. This would be important since generating a triangular signal is easier than a sinusoidal one.

It can be observed that for high values of vibration (> 45 Hz) the amplitude of the vibration gives rise to a low Vout value. Therefore, the **optimum operation region** for the sensor would be located within the range of **5** and **40 Hz**. Nonetheless, the response in all the cases follows an almost straight line, which indicates that the sensor has enough sensitivity to characterize the movement of the magnet.

Conclusions

An initial sensor prototype is proposed for the measurement of micrometric amplitude vibrations and acceleration for low frequency vibrating systems.

No difference was observed between exciting the wire with a triangular or sinusoidal signal facilitating the design for related electronics.

When analysing the response of the sensor to the frequencies between 5 and 50 Hz it is shown that the relation between the amplitude of the movement and the voltage of the sensor, the relation is linear. This would allow to use the sensor in all these frequencies, nonetheless, the optimal values are 5 and 40 Hz.

Wire sensor shows higher *GMI* effect under H_{dc}, leading in principle to a higher sensitivity for the sensor prototype.

This higher sensitivity of the wire was confirmed under non homogeneous magnetic field H_m. Nevertheless, both samples exhibit capability of measuring micrometric variations of distance.

Some other aspects that may need to be studied is the constancy of the V_{out} of the sensor (Peak-Peak) for different frequencies when the same acceleration is applied to the magnet.

Bibliography

[1] P. Ripka y K. Zaveta, «Magnetic Sensors: Principles and Applications,» *Handbook of Magnetic Materials.,* vol. 18, p. 347–420, 2009.

[2] A. Zhukov y V. Zhukova, «In magnetic properties and applications of ferromagnetic microwires with amorphous and nanocrystalline structure,» Nova Science Publishers Hauppauge, NY, nº 1-162, 2009.

[3] M. H. Phan y H. X. Peng, «Giant magnetoimpedance materials: Fundamentals and applications,» *Materials Science,* vol. 53, pp. 323-420, 2008.

[4] E. P. Harrison, G. L. Turney, H. Rowe y H. Gollop, «The electrical properties of high permeability wires carrying alternating current,» *Proceedings of the Royal Society of London,* vol. 891, pp. 451-479, 1936.

[5] B. Cullity y C. Graham, «Introduction to magnetic materials.,» Wiley, 2008.

[6] M. Hagiwara, A. Inoue y T. Masumoto, «Mechanical properties of Fe-Si-B amorphous wires produced by in-rotating-water spinning method,» Metallurgical Transactions A, vol. 13, nº 3, pp. 373-382, 1982.

[7] I. Ohnaka, T. Fukusako y T. Matui, «Preparation of amorphous wires,» journal japanese institute metals, vol. 45, pp. 751-762, 1981.

[8] M. H. Phan, Y. S. Kim, N. X. Chien, S. C. Yu, H. Lee y N. Chau, «Giant Magnetoimpedance Effect in Co70Fe5Si15B10 and Co70Fe5Si15Nb2.2Cu0.8B7 Ribbons,» Jpn J Apply Phys, vol. 42, nº 5571-5574, 2003.

[9] A. I. M. Hagiwara: y T. Masumoto, «Mechanical Properties of Fe-Si-B Amorphous Wires Produced by In-Rotating-Water Spinning Method,» Metall. Trans. A, vol. 13A, pp. 373-382, 1982.

[9] J. J. Beato-López, «Desarrollo de sensores basados en el efecto de magneto impedancia gigante empleando materiales magnéticos amorgos obtenidos mediante técnicas de enfriamiento ultrarrápido», tesis doctoral, Univ. Púb. Navarra, 2019.

Annex charts

F(kHz)	H=0 (mV)	Hmax (mV)	ΔZ/Z
100	329	177	85.8757062
150	364	176	106.818182
200	404	179	125.698324
250	428	182	135.164835
300	456	186	145.16129
350	483	192	151.5625
400	503	197	155.329949
450	525	202	159.90099
500	545	208	162.019231
550	567	216	162.5
600	585	223	162.331839
650	600	230	160.869565
700	622	236	163.559322
750	633	243	160.493827
800	650	250	160
850	668	258	158.914729
900	684	266	157.142857
950	700	274	155.474453
1000	717	284	152.464789

Data 1 Characterization in frequency of a ribbon with a current of 10 mA.

Iac (mA)	H=0 (mV)	Z (Ω)
5	262	52.4
5.5	294	53.4545455
6	325	54.1666667
6.5	358	55.0769231
7	393	56.1428571
7.5	429	57.2
8	461	57.625
8.5	498	58.5882353
9	532	59.1111111
9.5	567	59.6842105
10	601	60.1
10.5	630	60
11	663	60.2727273
11.5	693	60.2608696
12	723	60.25
12.5	754	60.32
13	780	60
13.5	808	59.8518519
14	832	59.4285714
14.5	862	59.4482759
15	885	59

Data 2 Swept in current with the optimum frequency of a ribbon: 700 kHz.

F(kHz)	H=0 (mV)	Hmax (mV)	ΔZ/Z
100	100	88	13.6363636
150	104	86	20.9302326
200	108	89	21.3483146
250	113	91	24.1758242
300	122	95	28.4210526
350	128	100	28
400	136	107	27.1028037
450	142	111	27.9279279
500	150	115	30.4347826
550	155	122	27.0491803
600	163	130	25.3846154
650	170	135	25.9259259
700	178	142	25.3521127
750	183	151	21.192053
800	191	155	23.2258065
850	204	162	25.9259259
900	200	167	19.760479
950	206	175	17.7142857
1000	211	180	17.2222222

Data 3 Characterization of the second ribbon with a current of 10 mA.

Iac (mA)	H=0 (mV)	Z (Ω)
5	75	15
5.5	83	15.0909091
6	87	14.5
6.5	96	14.7692308
7	103	14.7142857
7.5	110	14.6666667
8	118	14.75
8.5	125	14.7058824
9	132	14.6666667
9.5	142	14.9473684
10	148	14.8
10.5	154	14.6666667
11	161	14.6363636
11.5	171	14.8695652
12	178	14.8333333
12.5	186	14.88
13	195	15
13.5	200	14.8148148
14	209	14.9285714
14.5	217	14.9655172
15	225	15
47	846	18
67	1219.4	18.2
72.44	1318.408	18.2
77.8	1415.96	18.2
79.2	1488.96	18.8
85	1555.5	18.3
90	1638	18.2
102	1846.2	18.1
107	1931.35	18.05

Data 4 Swept in current with the optimum frequency of the ribbon: 500 kHz.

I(A)	H(kA/m)
0	0.14
0.02	0.18
0.04	0.214
0.08	0.283
0.1	0.317
0.14	0.387
0.19	0.47
0.25	0.573
0.3	0.655
0.33	0.707
0.39	0.81
0.44	0.903
0.47	0.961
0.51	1.029
0.6	1.182
0.67	1.299
0.73	1.401
1.24	2.298

Data 5 Characterization of the solenoid.

Is(A)	H(I) (A/m)	Vac(mV)	Iac(mA)	Z (Ω)
0	141	1473	79.2	18.5984848
0.03	193.017	1425	79.8	17.8571429
0.05	227.695	1408	79.9	17.6220275
0.08	279.712	1392	80	17.4
0.12	349.068	1368	80.2	17.0573566
0.17	435.763	1350	80.35	16.8014935
0.71	1372.069	1222	80.7	15.1425031
1.03	1926.917	1175	80.72	14.5564916
1.51	2759.189	1120	80.85	13.8528139
2.01	3626.139	1080	80.95	13.3415689
3.01	5360.039	1018	80.9	12.5834363
4	7076.6	979	81.5	12.0122699
4.98	8775.822	948	81.6	11.6176471
5.98	10509.722	930	81.6	11.3970588
7	12278.3	918	81.6	11.25
8.01	14029.539	910	81.65	11.1451317
8.97	15694.083	905	81.4	11.1179361
9.99	17462.661	900	81.5	11.0429448

Data 6 Values of the magnetic field and the impedance of a sample with the shape of a ribbon.

F(kHz)	H=0	Hmax	ΔZ/Z
100	83	69	20.2898551
150	88	71	23.943662
200	92	73	26.0273973
250	98	78	25.6410256
300	103	82	25.6097561
350	106	87	21.8390805
400	111	94	18.0851064
450	115	100	15
500	120	105	14.2857143
550	127	112	13.3928571
600	132	119	10.9243697
650	140	126	11.1111111
700	145	130	11.5384615
750	149	139	7.1942446
800	156	145	7.5862069
850	162	152	6.57894737
900	167	160	4.375
950	174	165	5.45454545
1000	180	173	4.04624277

Data 7 Characterization of a ribbon of PC-16 with a current of 10 mA.

Iac (mA)	H=0	Z
25	237	9.48
30	289	9.63333333
35	342	9.77142857
37.5	364	9.70666667
40	390	9.75
42.5	415	9.76470588
45	444	9.86666667
47.5	465	9.78947368
50	491	9.82
55	535	9.72727273
60	582	9.7
65	630	9.69230769

Data 8 Swept in current with the optimum frequency of the material: 200 kHz for a ribbon of PC-16.

Longitud de 3 cm		
H0 (mV)	Hmax (mV)	ΔZ/Z
421	307	0.3713355
Longitud de 5 cm		
H0 (mV)	Hmax (mV)	ΔZ/Z
633	413	0.53268765
Longitud de 7 cm		
H0 (mV)	Hmax (mV)	ΔZ/Z
805	506	0.59090909
Longitud de 9 cm		
H0 (mV)	Hmax (mV)	ΔZ/Z
1730	1160	0.49137931

Data 9 Relative variation of the impedance for several ribbon of PC-16 with lengths of 3,5,7 and 9 cm.

Is	H(I)	Vac(mV)	Iac(mA)	Z(Ω)
0	141	775	44.8	17.2991071
0.05	227.695	752	44.98	16.7185416
0.1	314.39	740	45.13	16.3970751
0.14	383.746	730	45.28	16.1219081
0.19	470.441	720	45.4	15.8590308
0.22	522.458	714	45.45	15.709571
0.31	678.509	701	45.51	15.4032081
0.35	747.865	692	45.7	15.1422319
0.39	817.221	687	45.87	14.9771092
0.55	1094.645	667	45.68	14.6015762
0.69	1337.391	656	45.7	14.3544858
0.82	1562.798	642	45.86	13.9991278
0.91	1718.849	637	45.7	13.9387309
0.99	1857.561	625	45.7	13.6761488
1.19	2204.341	608	45.7	13.3041575
1.99	3591.461	566	45.7	12.3851204
3.02	5377.378	538	45.9	11.7211329
3.96	7007.244	520	46	11.3043478
4.99	8793.161	510	45.9	11.1111111
6	10544.4	503.6	46	10.9478261
7.04	12347.656	500	46.2	10.8225108
7.97	13960.183	498	46	10.826087
9.06	15850.134	496	46	10.7826087
9.96	17410.644	495	46.1	10.7375271

Data 10 Values of the magnetic field and the impedance of a ribbon sample of 7 cm of PC-16.

Face A (kA/m)	30.25
Face B (kA/m)	91.4
Face C (kA/m)	35.36

Data 11 Magnetic field in the surface of each of the sides of the magnet.

x (cm)	H (kA/m)
0	91.4
1	17.6
2	3.478
3	1.24
4	0.52
5	0.186
6	0.056
7	0.021
8	0

Data 12 Magnetic field of side B of the magnet for each centimetre.

Distance (cm)	Voltage (mV)	ΔV (mV)
0	322.2	
		3.24
0.5	325.44	
		3.34
1	328.78	
		2.81
1.5	331.59	
		2.42
2	334.01	
		2.18
2.5	336.19	
		2.08
3	338.27	
		1.95
3.5	340.22	
		1.9
4	342.12	
		2.17
4.5	344.29	
		1.51
5	345.8	
		1.66
5.5	347.46	
		1.75
6	349.21	
		1.55
6.5	350.76	
		1.63
7	352.39	
		1.61
7.5	354	
		1.44
8	355.44	
		1.48
8.5	356.92	
		1.38
9	358.3	
		1.3
9.5	359.6	
		1.01
10	360.61	

Data 13 Variation of the voltage of the ribbon of 7 cm sample for every displacement of the magnet of 0.5 cm.

Distance (cm)	Voltage (mV)	ΔV (mV)
0	322.3	
		0.72
0.1	323.02	
		0.76
0.2	323.78	
		0.57
0.3	324.35	
		0.58
0.4	324.93	
		0.39
0.5	325.32	
		0.52
0.6	325.84	
		0.77
0.7	326.61	
		0.67
0.8	327.28	
		0.46
0.9	327.74	
		0.47
1	328.21	
		0.3
1.1	328.51	
		0.52
1.2	329.03	
		0.58
1.3	329.61	
		0.51
1.4	330.12	
		0.55
1.5	330.67	
		0.32
1.6	330.99	
		0.69
1.7	331.68	
		0.38
1.8	332.06	
		0.56
1.9	332.62	
		0.27
2	332.89	

Data 14 Variation of the voltage of the ribbon of 7 cm sample for every displacement of the magnet of 0.1 cm.

Distance (cm)	Voltage (mV)	ΔV (mV)
0.6	326.25	
		-0.02
0.61	326.23	
		0.06
0.62	326.29	
		0.05
0.63	326.34	
		0.05
0.64	326.39	
		0.06
0.65	326.45	
		0.06
0.66	326.51	
		0.08
0.67	326.59	
		0.05
0.68	326.64	
		0.08
0.69	326.72	
		0.03
0.7	326.75	

Data 15 Variation of the voltage of the ribbon of 7 cm sample for every displacement of the magnet of 0.01 cm.

Distance (cm)	Voltage (mV)	ΔV (mV)
0	138.99	
		1.68
0.5	140.67	
		1.63
1	142.3	
		1.4
1.5	143.7	
		1.02
2	144.72	
		0.83
2.5	145.55	
		0.7
3	146.25	
		0.65
3.5	146.9	
		0.52
4	147.42	
		0.43
4.5	147.85	
		0.44
5	148.29	
		0.37
5.5	148.66	
		0.41
6	149.07	
		0.34
6.5	149.41	
		0.28
7	149.69	
		0.34
7.5	150.03	
		0.41
8	150.44	
		0.42
8.5	150.86	
		0.4
9	151.26	
		0.34
9.5	151.6	
		0.29
10	151.89	

Data 16 Variation of the voltage of the ribbon of 3 cm sample for every displacement of the magnet of 0.5 cm.

Distance (cm)	Voltage (mV)	ΔV (mV)
0	138.95	
		0.35
0.1	139.3	
		0.38
0.2	139.68	
		0.37
0.3	140.05	
		0.39
0.4	140.44	
		0.26
0.5	140.7	
		0.34
0.6	141.04	
		0.28
0.7	141.32	
		0.28
0.8	141.6	
		0.29
0.9	141.89	
		0.26
1	142.15	
		0.34
1.1	142.49	
		0.33
1.2	142.82	
		0.19
1.3	143.01	
		0.3
1.4	143.31	
		0.23
1.5	143.54	
		0.29
1.6	143.83	
		0.24
1.7	144.07	
		0.16
1.8	144.23	
		0.16
1.9	144.39	
		0.18
2	144.57	

Data 17 Variation of the voltage of the ribbon of 3 cm sample for every displacement of the magnet of 0.1 cm.

Distancia (cm)	Tensión (mV)	ΔV (mV)
0.3	139.7	
		0.03
0.302	139.73	
		-0.01
0.304	139.72	
		0
0.306	139.72	
		0.02
0.308	139.74	
		0.01
0.31	139.75	
		0.01
0.312	139.76	
		0.01
0.314	139.77	
		0.01
0.316	139.78	
		0.03
0.318	139.81	
		0.04
0.32	139.85	
		0.02
0.322	139.87	
		0.01
0.324	139.88	
		0
0.326	139.88	
		0.02
0.328	139.9	
		0
0.33	139.9	
		0
0.332	139.9	
		0.01
0.334	139.91	
		-0.03
0.336	139.88	
		0.05
0.338	139.93	
		0.01
0.34	139.94	
		0.02
0.342	139.96	
		0.02

0.344	139.98	
		-0.01
0.346	139.97	
		-0.02
0.348	139.95	
		0.02
0.35	139.97	
		-0.01
0.352	139.96	
		-0.01
0.354	139.95	
		-0.08
0.356	139.87	
		0
0.358	139.87	
		0.01
0.36	139.88	
		0.03
0.362	139.91	
		0.03
0.364	139.94	
		0.01
0.366	139.95	
		0
0.368	139.95	
		0.01
0.37	139.96	
		0.01
0.372	139.97	
		0
0.374	139.97	
		0.01
0.376	139.98	
		0.01
0.378	139.99	
		0.01
0.38	140	
		0.01
0.382	140.01	
		0.01
0.384	140.02	
		0.02
0.386	140.04	
		0
0.388	140.04	

				0
0.39		140.04		
				0.01
0.392		140.05		
				0.01
0.394		140.06		
				0.01
0.396		140.07		
				0.01
0.398		140.08		
				0.02
0.4		140.1		

Data 18 Variation of the voltage of the ribbon of 3 cm sample for every displacement of the magnet of 0.002 cm.

F(kHz)	V H0	V Hmax	ΔZ/Z
50	235	133	76.6917293
100	263	127	107.086614
150	294	130	126.153846
200	304	128	137.5
250	319	136	134.558824
300	333	140	137.857143
350	346	144	140.277778
400	355	147	141.496599
450	370	159	132.704403
500	379	164	131.097561
550	390	168	132.142857
600	396	171	131.578947
650	406	175	132
700	413	185	123.243243
750	420	198	112.121212
800	427	204	109.313725
850	434	212	104.716981
900	447	220	103.181818
950	457	228	100.438596
1000	461	233	97.8540773

Data 19 Characterization of a wire of PC-17 with a current of 10 mA.

Iac	V H0	Z=V/I
2	52	26
2.5	70	28
3	85	28.3333333
3.5	101	28.8571429
4	120	30
4.5	131	29.1111111
5	150	30
5.5	168	30.5454545
6	181	30.1666667
6.5	201	30.9230769
7	217	31
7.5	237	31.6
8	261	32.625
8.5	277	32.5882353
9	298	33.1111111
9.5	322	33.8947368
10	343	34.3
10.5	369	35.1428571
11	390	35.4545455
11.5	411	35.7391304
12	436	36.3333333
12.5	458	36.64
13	476	36.6153846
13.5	499	36.962963
14	510	36.4285714
14.5	556	38.3448276
15	581	38.7333333
15.5	606	39.0967742
16	626	39.125
16.5	648	39.2727273
17	674	39.6470588
17.5	695	39.7142857
18	714	39.6666667
18.5	736	39.7837838
19	758	39.8947368
19.5	778	39.8974359
20	792	39.6
20.5	816	39.804878
21	833	39.6666667
21.5	854	39.7209302
22	872	39.6363636
22.5	889	39.5111111
23	907	39.4347826
23.5	922	39.2340426

Data 20 Swept in current with the optimum frequency of the material: 400 kHz for a wire of PC-17.

Is	H(I)	Vac(mV)	Iac(mA)	Z(Ω)
0	141	819	19.5	42
0.04	210.356	780	19.96	39.0781563
0.08	279.712	741	20.15	36.7741935
0.11	331.729	714	20.35	35.0859951
0.14	383.746	701	20.43	34.3122859
0.18	453.102	679	20.49	33.1381162
0.22	522.458	658	20.66	31.8489835
0.24	557.136	643	20.71	31.047803
0.29	643.831	629	20.77	30.2840636
0.33	713.187	596	20.85	28.5851319
0.45	921.255	576	20.97	27.4678112
0.52	1042.628	555	21.03	26.3908702
0.59	1164.001	513	21.15	24.2553191
0.75	1441.425	500	21.06	23.7416904
0.88	1666.832	478	21.02	22.7402474
1.01	1892.239	413	21.22	19.462771
1.48	2707.172	375	21.3	17.6056338
1.99	3591.461	354	21.21	16.6902405
2.47	4423.733	340	21.27	15.9849553
3.84	6799.176	313	21.45	14.5920746
4.93	8689.127	302	21.55	14.0139211
5.81	10214.959	298	21.53	13.8411519
6.92	12139.588	294	21.47	13.6935259
8.19	14341.641	290	21.52	13.4758364
9.28	16231.592	289	21.43	13.4857676
9.86	17237.254	288	21.54	13.3704735
-0.01	123.661	811	19.5	41.5897436
-0.02	106.322	800	19.66	40.6917599
-0.06	36.966	750	20.03	37.4438342
-0.08	2.288	729	20.13	36.2146051
-0.1	-32.39	715	20.31	35.2043328
-0.12	-67.068	704	20.34	34.6116028
-0.15	-119.085	688	20.43	33.6759667
-0.19	-188.441	671	20.45	32.8117359
-0.2	-205.78	667	20.51	32.5207216
-0.22	-240.458	659	20.41	32.2880941
-0.25	-292.475	649	20.63	31.4590402
-0.28	-344.492	640	20.63	31.0227824
-0.32	-413.848	628	20.6	30.4854369
-0.34	-448.526	622	20.74	29.9903568
-0.36	-483.204	615	20.69	29.7245046
-0.39	-535.221	609	20.71	29.406084
-0.41	-569.899	601	20.76	28.9499037
-0.44	-621.916	594	20.73	28.6541245

-0.46	-656.594	587	20.733	28.3123523
-0.48	-691.272	581	20.8	27.9326923
-0.51	-743.289	574	20.85	27.529976
-0.53	-777.967	568	20.85	27.2422062
-0.56	-829.984	559	20.93	26.7080745
-0.59	-882.001	546	20.87	26.161955
-0.63	-951.357	539	21.02	25.6422455
-0.66	-1003.374	533	21.05	25.3206651
-0.7	-1072.73	522	21.03	24.8216833
-0.75	-1159.425	508	21.14	24.0302744
-0.81	-1263.459	495	21	23.5714286
-0.85	-1332.815	488	21.1	23.1279621
-0.95	-1506.205	469	21.19	22.1330816
-1.02	-1627.578	458	21.24	21.5630885
-1.21	-1957.019	428	21.23	20.1601507
-1.41	-2303.799	406	21.23	19.1238813
-1.59	-2615.901	387	21.33	18.1434599
-1.8	-2980.02	372	21.34	17.4320525
-2	-3326.8	359	21.34	16.8228679
-2.47	-4141.733	338	21.41	15.7870154
-3	-5060.7	324	21.45	15.1048951
-3.57	-6049.023	315	21.36	14.747191
-4.04	-6863.956	308	21.38	14.4059869
-5	-8528.5	302	21.37	14.1319607
-6.02	-10297.078	297	21.42	13.8655462
-7.04	-12065.656	292	21.36	13.670412
-8.03	-13782.217	289	21.5	13.4418605
-9.23	-15862.897	287	21.56	13.3116883
-9.91	-17041.949	287	21.4	13.411215

Data 21 Values of the magnetic field and the impedance of a wire sample of 3 cm of PC-17 .

Distance (cm)	Voltage (mV)	ΔV (mV)
0	101.448	
		13.146
0.5	114.594	
		14.292
1	128.886	
		16.696
1.5	145.582	
		13.941
2	159.523	
		11.53
2.5	171.053	
		10.152
3	181.205	
		8.001
3.5	189.206	
		5.03
4	194.236	
		4.776
4.5	199.012	
		4.773
5	203.785	
		4.563
5.5	208.348	
		3.976
6	212.324	
		3.38
6.5	215.704	
		3.133
7	218.837	
		3.483
7.5	222.32	
		2.873
8	225.193	
		2.203
8.5	227.396	
		1.667
9	229.063	
		1.438
9.5	230.501	
		1.292
10	231.793	

Data 22 Variation of the voltage of the wire of 3 cm sample for every displacement of the magnet of 0.5 cm.

Distance (cm)	Voltage (mV)	ΔV (mV)
0.5	114.468	
		2.338
0.6	116.806	
		2.625
0.7	119.431	
		3.061
0.8	122.492	
		3.291
0.9	125.783	
		3.009
1	128.792	
		3.195
1.1	131.987	
		2.826
1.2	134.813	
		3.201
1.3	138.014	
		3.04
1.4	141.054	
		3.671
1.5	144.725	
		3.144
1.6	147.869	
		2.631
1.7	150.5	
		3.151
1.8	153.651	

Data 23 Variation of the voltage of the wire of 3 cm sample for every displacement of the magnet of 0.1 cm.

Distance (cm)	Voltage (mV)	ΔV (mV)
1.5	144.931	
		-0.07
1.498	144.861	
		-0.052
1.496	144.809	
		-0.069
1.494	144.74	
		-0.057
1.492	144.683	
		-0.059
1.49	144.624	
		-0.051
1.488	144.573	
		-0.067
1.486	144.506	
		-0.054
1.484	144.452	
		-0.087
1.482	144.365	
		-0.04
1.48	144.325	
		-0.052
1.478	144.273	
		-0.047
1.476	144.226	
		-0.076
1.474	144.15	
		-0.07
1.472	144.08	
		-0.075
1.47	144.005	
		-0.058
1.468	143.947	
		-0.044
1.466	143.903	
		-0.082
1.464	143.821	
		-0.058
1.462	143.763	
		-0.062
1.46	143.701	
		-0.051
1.458	143.65	
		-0.058

1.456	143.592	
		-0.082
1.454	143.51	
		-0.046
1.452	143.464	
		-0.079
1.45	143.385	
		-0.026
1.448	143.359	
		-0.098
1.446	143.261	
		-0.059
1.444	143.202	
		-0.067
1.442	143.135	
		-0.05
1.44	143.085	
		-0.051
1.438	143.034	
		-0.069
1.436	142.965	
		-0.075
1.434	142.89	
		-0.06
1.432	142.83	
		-0.054
1.43	142.776	
		-0.068
1.428	142.708	
		-0.057
1.426	142.651	
		-0.062
1.424	142.589	
		-0.058
1.422	142.531	
		-0.022
1.42	142.509	
		-0.061
1.418	142.448	
		-0.075
1.416	142.373	
		-0.081
1.414	142.292	
		-0.049
1.412	142.243	

		-0.086
1.41	142.157	
		-0.048
1.408	142.109	
		-0.053
1.406	142.056	
		-0.082
1.404	141.974	
		-0.07
1.402	141.904	
		-0.065
1.4	141.839	

Data 24 Variation of the voltage of the wire of 3 cm sample for every displacement of the magnet of 0.002 cm.